Technical Report

Analysis of the Performance of Innovative Mixtures

Client:
POLYMERTEAM NV
represented by its legal representative NOEL ESSERS

Address:
Via Calto, 731 - 45030 Ceneselli (RO)

Scientific Director:	Prof. Ing. Anna Laura Pisello
Technical–Operational Manager:	Ing. Claudia Fabiani
Measurement Execution and Data Processing	Ing. Francesco Marchini Ing. Silvia Cavagnoli Ing. Claudia Fabiani
Drafting of Technical Report:	Ing. Francesco Marchini Ing. Silvia Cavagnoli Ing. Claudia Fabiani
Final Technical–Scientific Review and General Supervision:	Prof. Ing. Anna Laura Pisello

Place and Issue Date: Perugia, **01/09/2025**

via Duranti 93
06125 Perugia
Anna Laura Pisello
075 585 3753
anna.pisello@unipg.it

Summary

via Duranti 93
06125 Perugia
Anna Laura Pisello
075 585 3753
anna.pisello@unipg.it

via Duranti 93
06125 Perugia
Anna Laura Pisello
075 585 3753
anna.pisello@unipg.it

1. Introduction

This report critically describes the results obtained from the experimental tests carried out on innovative mixtures designed for pavement applications aimed at promoting effective passive cooling. CIRIAF (Centro Interuniversitario di Ricerca sull'Inquinamento da Agenti Fisici – Interuniversity research centre on pollution and environment Mauro Felli) was commissioned by the client POLYMERTEAM Srl to perform the tests necessary to evaluate the thermo–optical characteristics of different sample types, with the objective of understanding how these materials influence surface overheating and affect the energy balance of urban spaces. The experimental activities were organized into three main work tasks:

- Evaluation of solar reflectance and thermal emittance properties, with subsequent calculation of the Solar Reflectance Index (SRI).
- Evaluation of thermal conductivity, thermal diffusivity, and specific heat capacity.
- Evaluation of surface overheating performance, air temperature, and radiation re-emitted by the surface.

via Duranti 93
06125 Perugia
Anna Laura Pisello
075 585 3753
anna.pisello@unipg.it

2. Materials and Samples

The materials analyzed consist of innovative mixtures developed by POLYMERTEAM Srl for the realization of outdoor pavements with high passive cooling capability. In collaboration with the Evizero brand, four solutions were produced, differing in color and intended for different outdoor applications. The sample types analyzed are shown in Figure 1 and are as follows:

(i) a white pavement sample, consisting of "Bianco Ancona" limestone aggregates with the addition of 1% white pigment and Evizero binder, a transparent, ecological, and innovative binder;

(ii) a yellow pavement sample, identical to (i) but without the addition of white pigment;

(iii) a red pavement sample, produced with a different type of aggregate, called "Rosso Verona," and the Evizero binder;

(iv) a black pavement sample, produced with the same aggregates as (i) and (ii) but with the addition of bitumen instead of the Evizero binder.

In this report, the samples will be referred to as follows: (i) White, (ii) Natural, (iii) Red, (iv) Black.

Figure 1. Types of samples analyzed

For each sample type, specimens were prepared in two different sizes, selected according to the type of thermo-optical analysis to be performed in the laboratory. These properties were examined both in the initial state (after production) and after exposing the samples to real environmental conditions (following an ageing period). To this end, all samples were placed on the CIRIAF rooftop (Figure 2) and left exposed for periods of 30, 60, and 90 days. This made it possible to evaluate the evolution of the main thermo-optical properties as a consequence of natural ageing.

via Duranti 93 06125 Perugia Anna Pisello Laura 075 585 3753 anna.pisello@unipg.it

Figure 2. Natural ageing of the samples.

More specifically, Table 1 reports the specifications of the different types of samples tested and the corresponding ageing durations.

Table 1. Characteristics of the samples and type of experimental analysis conducted.

	Experimental test	**Specimen geometry**	**Type of mixture**
1	Evaluation of solar reflectance and thermal emissivity with calculation of the Solar Reflectance Index (SRI): • Pre-ageing • 30-day ageing • 60-day ageing • 90-day ageing	• Cylindrical shape, thickness 2 cm, diameter 10 cm	• "White" sample • "Natural" sample • "Red" sample • "Black" sample
2	Evaluation of thermal conductivity, thermal diffusivity and specific heat capacity using the hot-disk method: • Pre-ageing • 30-day ageing • 60-day ageing • 90-day ageing	• Cylindrical shape, thickness 2 cm, diameter 10 cm	• "White" sample • "Natural" sample • "Red" sample • "Black" sample
3	Evaluation of surface overheating performance, air temperature and longwave radiation emitted by the surface (pre-ageing).	• Cylindrical shape, thickness 5 cm, diameter 15 cm	• "White" sample • "Natural" sample • "Red" sample • "Black" sample

via Duranti 93
06125 Perugia
Anna Pisello
Laura
075 585 3753
anna.pisello@unipg.it

3. Evaluation of Solar Reflectance, Thermal Emittance and Calculation of the Solar Reflectance Index (SRI).

One of the analyses carried out on the samples concerned the characterization of their optical and thermal properties, performed via spectrophotometry and portable emissometer measurements, respectively. From these analyses, the solar reflectance coefficient and the thermal emittance value were obtained and subsequently used as input data for determining the Solar Reflectance Index (SRI).

3.1 Optical Characterization

In order to determine the optical properties of the specimens in the solar spectrum and to evaluate the solar reflectance coefficients, experimental tests were carried out on 10-cm-diameter samples provided by POLYMERTEAM Srl. The measurements were performed at the Fisica Tecnica EAPLAB laboratory at CIRIAF using a PerkinElmer 1050+ spectrophotometer equipped with a 15-cm integrating sphere. For each sample, the test was conducted on three different points of the surface, allowing the subsequent calculation of mean values. The adopted methodology and the relevant reference standards are described in this section, together with the experimental results.

3.1.1 Reference Standards

- ASTM E903-12 (2020)
  Standard Test Method for Solar Absorptance, Reflectance, and Transmittance of Materials Using Integrating Spheres
- ASTM Standard G173
  Standard Tables for Reference Solar Spectral Irradiances
- ISO 9050:2003
  Glass in building - Determination of light transmittance, solar direct transmittance, total solar energy transmittance, ultraviolet transmittance and related glazing factors

3.1.2 Measurement Method

The standard described above defines the test method, which involves the use of a spectrophotometer equipped with an integrating sphere to measure the solar absorptance, reflectance and transmittance of a

via Duranti 93
06125 Perugia
Anna Laura Pisello
075 585 3753
anna.pisello@unipg.it

surface. These measurements are essential for evaluating the optical properties of materials in relation to their ability to reflect, transmit or absorb solar radiation, and are particularly useful in passive solar energy applications or for improving the energy efficiency of building materials. To determine the solar reflectance **R** of the surface under analysis, defined as the ratio between the reflected fraction and the total amount of incident solar radiation, the spectral reflectance **ρλ** of the surface is first measured over a wavelength range **λ** [nm] extending from 300 nm to 2500 nm. More than 99% of the solar radiation incident on the Earth's surface falls within this interval. Solar reflectance **R** is finally calculated as the average of the spectral reflectance weighted by the monochromatic solar irradiance at ground level, **Iλ** [W/(m²·nm)], as tabulated in ASTM Standard G173.

$$R = \frac{\int_{300}^{2500} \rho_\lambda(\lambda) \cdot I_\lambda(\lambda)\, d\lambda}{\int_{300}^{2500} I_\lambda(\lambda)\, d\lambda}$$

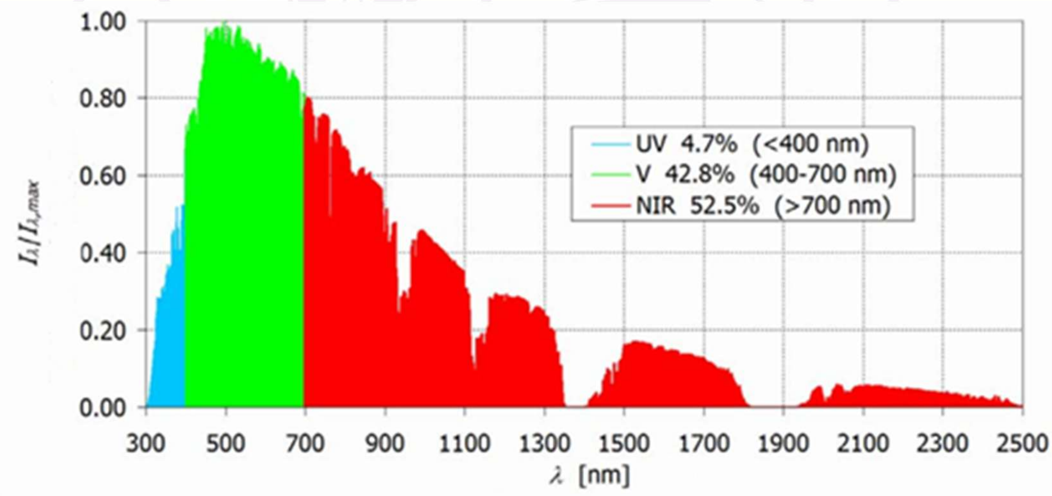

Figure 3. Normalized spectrum of solar radiation at the Earth's surface (ASTM Standard G173).

3.1.3 Procedure

The analysis of the optical properties for the evaluation of solar reflectance was carried out on the 10-cm-diameter, 2-cm-thick samples. The tests were performed over the entire solar spectrum, i.e., wavelengths between 300 and 2500 nm, acquiring solar reflectance data

via Duranti 93
06125 Perugia
Anna Pisello
Laura
075 585 3753
anna.pisello@unipg.it

with a resolution of 1 nm. Before performing the measurements, the instrument was calibrated using a certified reflectance standard (Spectralon), in order to ensure the accuracy of the results. For each type of sample, three measurements were carried out on three different points of the surface, and the corresponding mean values were calculated during the data-processing phase to determine the reflectance coefficients. The measurements were performed at multiple ageing stages: pre-ageing (time zero) and post-ageing (i.e., after 30, 60 and 90 days of outdoor exposure). This made it possible to evaluate the evolution of the optical characteristics under real ageing conditions.

3.1.4 Description of the Equipment

PerkinElmer LAMBDA 1050+ UV-Vis-NIR Spectrophotometer

Spectrophotometry is an analytical method used to study how a material interacts with electromagnetic radiation by measuring the intensity of light absorbed, transmitted or reflected as a function of wavelength. For this analysis, a PerkinElmer LAMBDA 1050+ UV/VIS/NIR spectrophotometer (Figure 4), was used. This is a high-performance instrument capable of analyzing a wide spectral range, including the ultraviolet (300–380 nm), the visible (381–780 nm) and the near infrared (781–2500 nm). The optical system includes a deuterium lamp for the UV region and a tungsten lamp for the visible and NIR regions. The generated light then strikes the surface of the sample positioned on the sample holder. The instrument is also equipped with a 15-cm-diameter Spectralon-coated integrating sphere, used to collect the light reflected in all directions from the sample and to ensure accurate measurement.

Figure 4. PerkinElmer LAMBDA 1050+ UV/Vis/NIR spectrophotometer.

via Duranti 93
06125 Perugia
Anna Pisello
Laura
075 585 3753
anna.pisello@unipg.it

3.1.5 Results

This section presents the results of the solar reflectance analysis for each sample examined. The reported data correspond to the average of three measurements performed on each sample at three different surface points. Specifically, the white sample is represented by grey-scale lines, the natural sample by yellow-toned lines, the red sample by red-scale lines, and the black sample by black-scale lines.

In particular, Figure 5 shows the results for all samples at time zero, i.e., before ageing. Analysis of the results shows that the white sample exhibits the highest solar reflectance, followed by the natural, red and black samples, respectively. However, in the UV spectral range, the natural sample shows the highest reflectance.

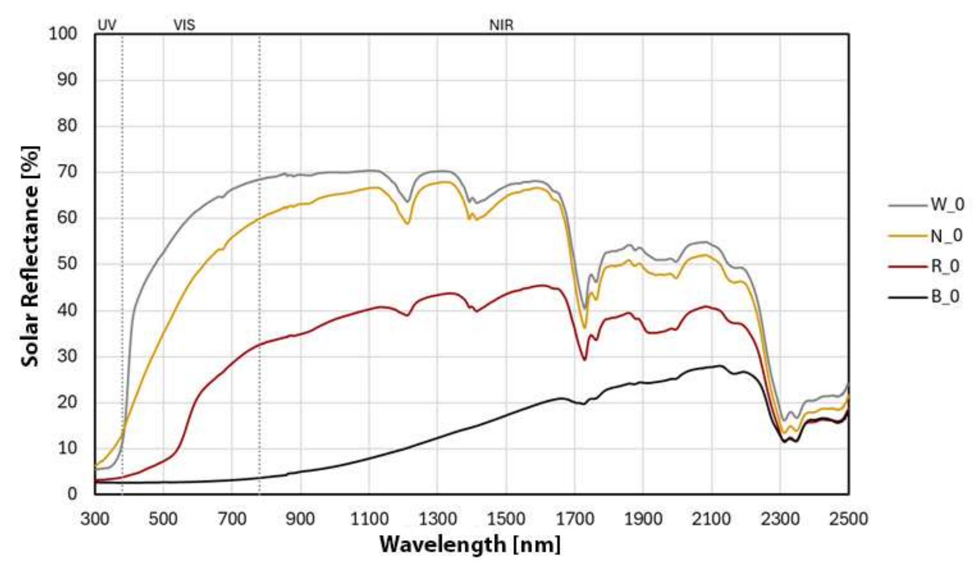

Figure 5. Comparison of solar reflectance curves of samples at time 0

This analysis was repeated on the same types of samples after 30, 60 and 90 days of natural ageing. Figure 6 presents a visual comparison between the samples before and after ageing, where a colour variation towards lighter tones can be observed when comparing the photos at 0 and 90 days.

via Duranti 93
06125 Perugia
Anna Pisello
Laura
075 585 3753
anna.pisello@unipg.it

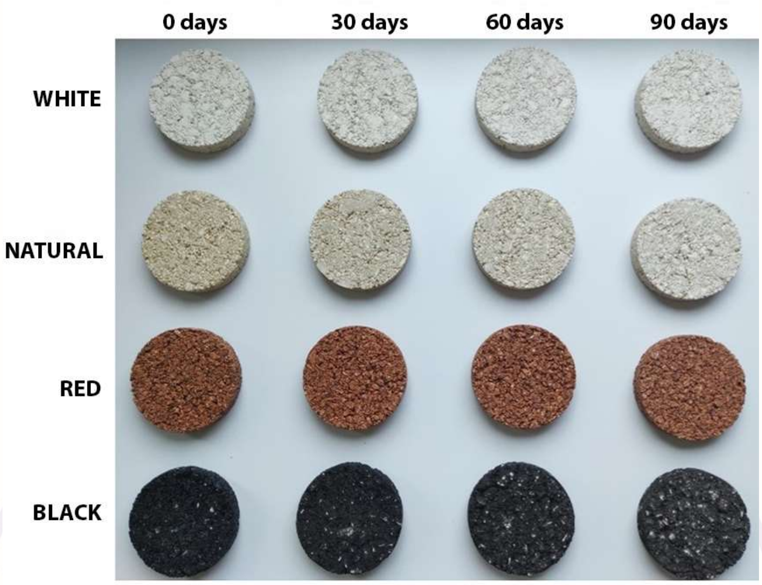

Figure 6. Macroscopic visual effect of exposure to atmospheric agents (natural aging) on samples

Figure 7 instead shows the results in terms of solar reflectance for each sample before and after ageing. For the white sample, ageing led to a reduction in solar reflectance compared with time zero; however, this decrease remained quite stable, with only minimal variation between 30 and 90 days.

The natural sample also shows a decrease in reflectance over time, particularly at wavelengths above 700 nm. Below this threshold, however, reflectance tends to increase with increasing ageing duration.

In the case of the red sample, ageing resulted in an increase in solar reflectance compared with time zero, with a more evident increase observed after 90 days of exposure.

For the black sample, an initial increase in reflectance is observed up to approximately 1100 nm in the samples aged for 30 and 60 days, followed by a decrease with respect to time zero. However, after 90 days of exposure, a new increase in reflectance is recorded, extending up to approximately 1500 nm.

via Duranti 93
06125 Perugia
Anna Pisello
Laura
075 585 3753
anna.pisello@unipg.it

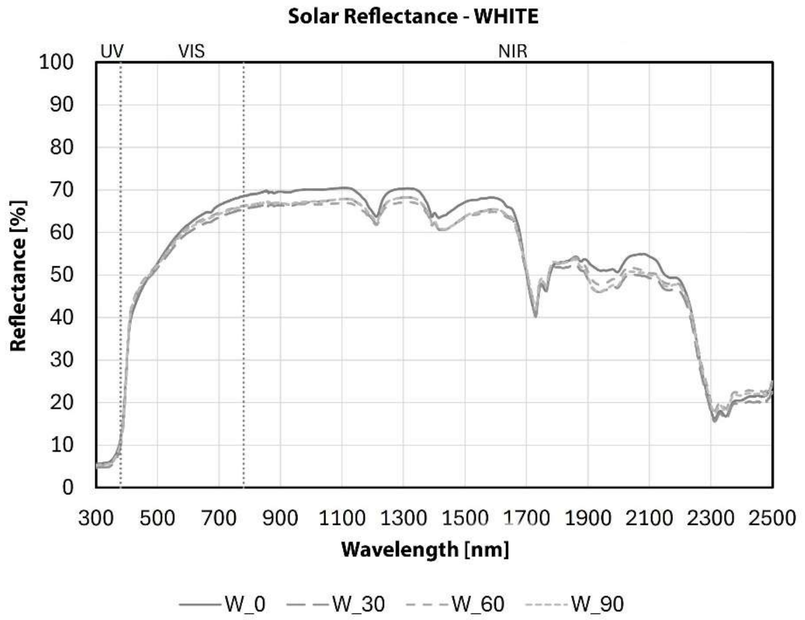

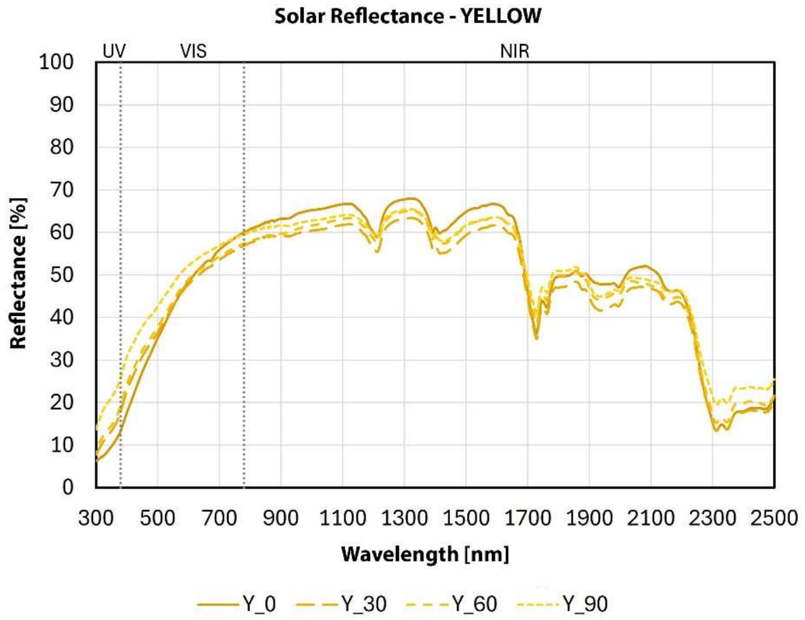

via Duranti 93
06125 Perugia
Anna Laura
Pisello
075 585 3753
anna.pisello@unipg.it

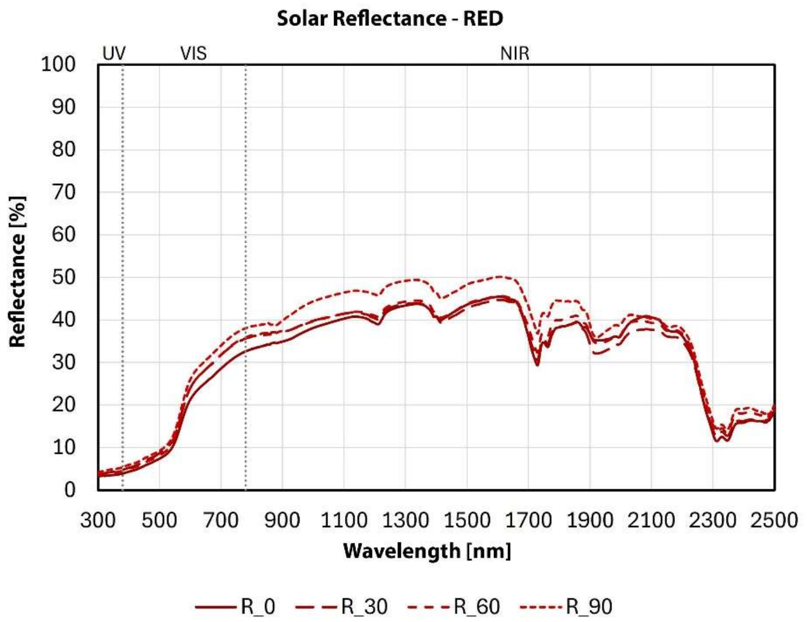

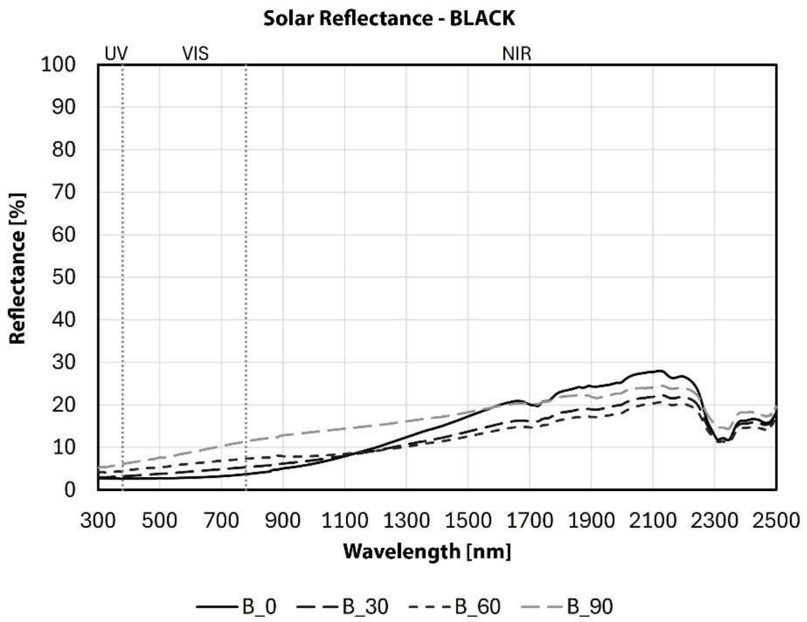

Figure 7. Solar reflectance of samples before and after the natural aging.

via Duranti 93
06125 Perugia
Anna Pisello
Laura
075 585 3753
anna.pisello@unipg.it

3.2 Thermal Characterization

This section reports the reference standards and analytical methods adopted for the thermal characterization of the samples under study. In particular, tests for the evaluation of thermal emittance were carried out using a Devices and Services AE1 portable emissometer on cylindrical samples with a diameter of 15 cm and a thickness of 5 cm.

3.2.1 Reference Standards

- ASTM C1371-04a
  Standard Test Method for Determination of Emittance of Materials Near Room Temperature Using Portable Emissometers.

3.2.2 Measurement Method

The measurement method described in ASTM C1371-04a specifies the procedures for determining the emittance of materials at room temperature using portable emissometers.

3.2.3 Procedure

Before performing the thermal emittance test, the portable emissometer is calibrated under the same environmental conditions in which the measurement is carried out, using two reference standards: one with high emittance (ε = 0.88) and one with low emittance (ε = 0.06). Once the instrument has been calibrated, the test is performed on the material, and the emittance value is obtained based on the calibration settings of the instrument.

3.2.4 Description of the Equipment Used

The instrument used for thermal emittance analysis is the AE1 portable emissometer manufactured by Devices & Services Company, serial number 2296, capable of measuring total hemispherical emittance at 65°C. The device includes a heated thermopile detector (Figure 8a), which creates a temperature difference between the detector and the surface, and a D&S Scaling RD1 digital voltmeter used as a readout unit. This features a gain-adjustment knob used to set the voltage corresponding to the emittance of the calibration standard (Figure 8.b). At the end of the test, the instrument provides a thermal emittance value for the

via Duranti 93
06125 Perugia
Anna Pisello
Laura
075 585 3753
anna.pisello@unipg.it

analyzed material between 0 and 1, with two decimal places. The detailed specifications of the instrument are reported in Table 2.

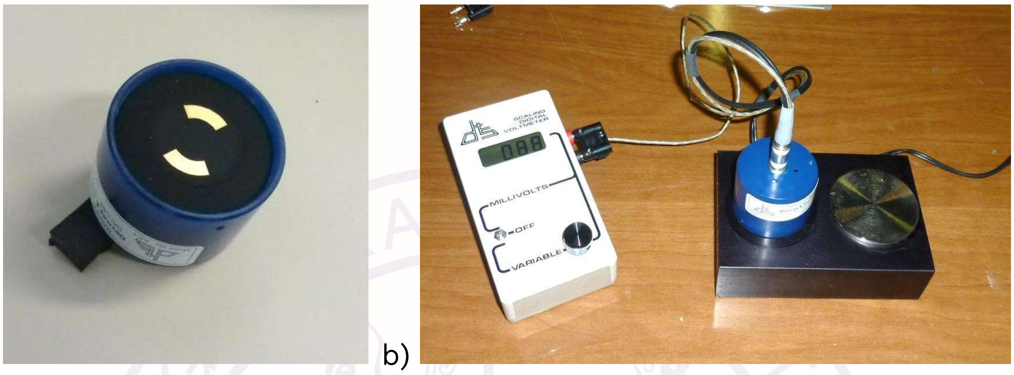

a) b)

Figure 8. Differential thermopile detector (a) and calibration procedure.

Table 2. Specifications of the portable emissometer.

Battery	Up to 12 hours of continuous operation
Power supply	100-240V, 50-60 Hz, 12V DC
Output	2.4 mV
Warm-up time	30 minutes
Reproducibility	+/- 0.01 emissivity units
Calibration standards	ε = 0.06; ε = 0.88
Adapters	AE-AD1: flat materials with a minimum diameter of 3,8 cm AE-AD3: flat materials with a minimum diameter of 2,54 cm AE-ADP: flat materials with a minimum diameter of 3,8 cm and low thermal conductivity, cylindrical surfaces with a large radius (>2 inches), and rough or textured surfaces.

3.2.5 Results

This section presents the results of the thermal emittance analysis of the four different types of samples analyzed, namely white, natural, red and black. The tests were carried out both before and after natural ageing. The ageing process led to slight improvements in thermal emittance for some sample types as exposure time increased, while for the black sample, for instance, no change was observed. The results are reported in Table 3.

via Duranti 93
06125 Perugia
Anna Pisello
Laura
075 585 3753
anna.pisello@unipg.it

Table 3. Thermal emissivity values collected with the portable emissometer.

	Thermal emissivity			
	0 days	30 days	60 days	90 days
White	0.94	0.95	0.96	0.96
Natural	0.93	0.94	0.96	0.96
Red	0.96	0.98	0.98	0.98
Black	0.96	0.96	0.96	0.96

3.3 Calculation of the Solar Reflectance Index (SRI)

The Solar Reflectance Index (SRI) expresses the ability of a material to reflect solar energy and release absorbed heat, indicating how "cool" a material remains when exposed to sunlight. The SRI combines solar reflectance and thermal emittance values to quantify the ability of a surface to reflect solar radiation and dissipate absorbed heat. High SRI values correspond to greater passive-cooling effectiveness and contribute to mitigating the urban heat island effect. Conventionally, a standard black surface has an SRI of 0 and a standard white surface an SRI of 100; however, depending on material properties, the index may assume values lower than 0 or higher than 100.

3.3.1 Reference Standards

- ASTM E1980-11(2019)
  Standard Practice for Calculating Solar Reflectance Index of Horizontal and Low-Sloped Opaque Surfaces

3.3.2 Calculation Method

The Solar Reflectance Index is calculated according to ASTM E1980-11 and combines the solar reflectance and thermal emittance of the material. These parameters are directly related to the surface temperature of the sample, as they represent, respectively, the effect of solar radiation on the surface and the ability of the surface to re-emit absorbed energy. The standard provides two different approaches for calculating SRI. The first approach determines the steady-state surface temperature (T_S) reached by the material under specified environmental conditions of solar irradiance and ventilation defined in ASTM E1980-11 (solar flux equal to 1000 W/m², outdoor air temperature equal to 310 K and sky temperature equal to 300 K, with three ventilation levels). The

via Duranti 93
06125 Perugia
Anna Pisello
Laura
075 585 3753
anna.pisello@unipg.it

steady-state surface temperature (T_S) of a material exposed to solar irradiance and airflow is determined by the energy balance between the energy absorbed and the energy dissipated by the material. Under steady-state conditions, the solar energy absorbed by the surface equals the energy lost through thermal radiation and convection to the environment. Based on the calculated T_S value, the SRI is obtained as follows,

$$SRI = 100 \cdot \frac{(T_{white} - T_s)}{(T_{black} - T_{white})}$$

where T_{white} and T_{black} are the limiting surface temperatures corresponding to a reference white surface (solar reflectance factor 0.8 – emittance 0.9 – SRI = 100 under standard environmental conditions) and a reference black surface (solar reflectance factor 0.05 – emittance 0.9 – SRI = 0 under standard environmental conditions), respectively, under the same conditions used to determine T_s.

In the second approach described in the standard, the SRI value is determined from the following equation:

$$SRI = 123.97 - 141.35\chi + 9.655\chi^2$$

where:

$$\chi = \frac{((1 - r) - 0.029\varepsilon)\,(8.797 + h_c)}{9.5205\varepsilon + h_c}$$

where r and ε represent the measured solar reflectance and thermal emittance, respectively). The term $\mathbf{h_c}$ is the convective heat transfer coefficient, which according to the standard may assume three different values: 5, 12 and 30 W/m²K, corresponding to different wind-speed conditions (0–2 m/s, 2–6 m/s and 6–10 m/s, respectively).

3.3.3 Results

In this section, the results of the SRI calculation for the samples before and after aging are presented. Table 4 reports the data at time 0, i.e., before aging. The sample with the highest SRI value is the white one, followed by the natural, red, and black samples. In particular, the white sample also exhibits the lowest surface temperatures, which tend to decrease with increasing convective heat transfer coefficient h_c.

via Duranti 93 06125 Perugia Anna Laura Pisello 075 585 3753 anna.pisello@unipg.it

Conversely, the black sample shows the lowest SRI value, with surface temperatures exceeding 100°C for h_c = 5 W/m²K.

Table 4. Calculation of global coefficients and SRI index – Initial values (0 days).

Sample	Convective heat transfer coefficient (W/m² K)	Solar reflectance	Thermal emissivity	SRI	Surface temperature (°C)	Surface temperature of white reference sample (°C)	Surface temperature of black reference sample (°C)
White	h = 5	0.59	0.94	71	65.3	49.3	103.7
	h = 12	0.59	0.94	72	55.3	44.6	82.5
	h = 30	0.59	0.94	73	46.4	40.8	61.1
Natural	h = 5	0.50	0.93	57	72.5	49.3	103.7
	h = 12	0.50	0.93	59	60.2	44.6	82.5
	h = 30	0.50	0.93	60	49	40.8	61.1
Red	h = 5	0.25	0.96	28	88.4	49.3	103.7
	h = 12	0.25	0.96	28	71.7	44.6	82.5
	h = 30	0.25	0.96	28	55.3	40.8	61.1
Black	h = 5	0.06	0.96	6	100.7	49.3	103.7
	h = 12	0.06	0.96	4	80.8	44.6	82.5
	h = 30	0.06	0.96	3	60.4	40.8	61.1

During the aging period, the various optical and thermal coefficients underwent variations, and the corresponding SRI results are reported in

Table 5, Table 6 e Table 7. In general, the SRI tends to increase with the aging period, with the exception of the white sample, for which a slight reduction is observed. Nevertheless, the white sample remains the one with the highest SRI in all cases.

Table 5. Calculation of global coefficients and SRI index – 30 days

Sample	Convective heat transfer coefficient (W/m² K)	Solar reflectance	Thermal emissivity	SRI	Surface temperature (°C)	Surface temperature of white reference sample (°C)	Surface temperature of black reference sample (°C)
White	h = 5	0.57	0.95	68	66.4	49.3	103.7
	h = 12	0.57	0.95	70	56.1	44.6	82.5
	h = 30	0.57	0.95	70	46.8	40.8	61.1
Natural	h = 5	0.48	0.94	56	73.3	49.3	103.7
	h = 12	0.48	0.94	57	60.8	44.6	82.5

via Duranti 93 06125 Perugia Anna Laura Pisello 075 585 3753 anna.pisello@unipg.it

	h = 30	0.48	0.94	58	49.3	40.8	61.1
Red	h = 5	0.27	0.98	31	86.7	49.3	103.7
	h = 12	0.27	0.98	31	70.6	44.6	82.5
	h = 30	0.27	0.98	31	54.8	40.8	61.1
Black	h = 5	0.06	0.96	6	100.3	49.3	103.7
	h = 12	0.06	0.96	5	80.6	44.6	82.5
	h = 30	0.06	0.96	4	60.3	40.8	61.1

Table 6. Calculation of global coefficients and SRI index – 60 days.

Sample	Convective heat transfer coefficient (W/m² K)	Solar reflectance	Thermal emissivity	SRI	Surface temperature (°C)	Surface temperature of white reference sample (°C)	Surface temperature of black reference sample (°C)
White	h = 5	0.58	0.96	70	65.8	49.3	103.7
	h = 12	0.58	0.96	71	55.7	44.6	82.5
	h = 30	0.58	0.96	71	46.6	40.8	61.1
Natural	h = 5	0.49	0.96	58	72	49.3	103.7
	h = 12	0.49	0.96	59	60	44.6	82.5
	h = 30	0.49	0.96	60	48.9	40.8	61.1
Red	h = 5	0.27	0.98	31	86.6	49.3	103.7
	h = 12	0.27	0.98	31	70.5	44.6	82.5
	h = 30	0.27	0.98	31	54.8	40.8	61.1
Black	h = 5	0.08	0.96	7	99.6	49.3	103.7
	h = 12	0.08	0.96	6	80	44.6	82.5
	h = 30	0.08	0.96	5	60	40.8	61.1

Table 7. Calculation of global coefficients and SRI index – 90 days.

Sample	Convective heat transfer coefficient (W/m² K)	Solar reflectance	Thermal emissivity	SRI	Surface temperature (°C)	Surface temperature of white reference sample (°C)	Surface temperature of black reference sample (°C)
White	h = 5	0.58	0.96	70	65.7	49.3	103.7
	h = 12	0.58	0.96	71	55.7	44.6	82.5
	h = 30	0.58	0.96	71	46.6	40.8	61.1
Natural	h = 5	0.52	0.96	62	69.8	49.3	103.7
	h = 12	0.52	0.96	63	58.5	44.6	82.5
	h = 30	0.52	0.96	64	48.1	40.8	61.1
Red	h = 5	0.30	0.98	34	85	49.3	103.7
	h = 12	0.30	0.98	35	69.4	44.6	82.5
	h = 30	0.30	0.98	34	54.1	40.8	61.1

via Duranti 93 06125 Perugia Anna Pisello Laura 075 585 3753 anna.pisello@unipg.it

Black	h = 5	0.11	0.96	12	97.3	49.3	103.7
	h = 12	0.11	0.96	11	78.3	44.6	82.5
	h = 30	0.11	0.96	10	59	40.8	61.1

Figure 9 shows the SRI results of the samples for h_c = 12 W/m²K. From the graph, it can be observed that, with the exception of the black sample and the red sample before aging, the analyzed materials exhibit SRI values higher than the requirement set by D.M. 05/08/2024 – Paragraph 2.2.1 (SRI ≥ 29) for exterior surfaces. This indicates the potential applicability of these materials for outdoor pavement surfaces.

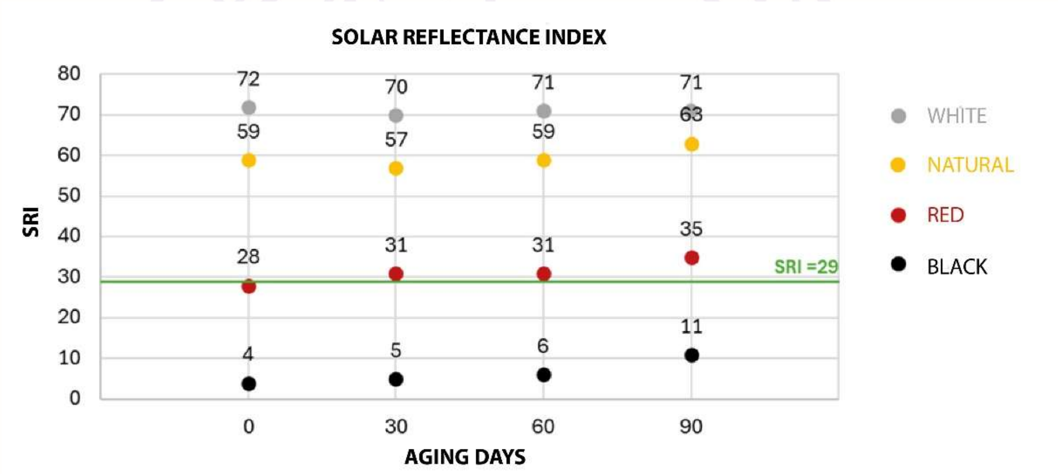

Figure 9. SRI with h_c = 12 W/m² K

4. Evaluation of the thermal conductivity, thermal diffusivity, and specific heat capacity

4.1 Thermal characterization

In this section, the thermal characterization of the samples before and after the aging period is presented. The measurements were carried out using the Transient Plane Source (TPS) method with the Hot Disk 2500 S instrument. Through this analysis, it was possible to determine the thermal conductivity [W/(mK)], thermal diffusivity [mm²/s], and volumetric specific heat capacity [MJ/(m³K)].

4.1.1 Reference standards

- UNI EN ISO 22007-2:2015
  Plastics – Determination of thermal conductivity and thermal diffusivity – Part 2: Transient plane heat source (hot disk) method.
- UNI CEI 70098-3:2016
  Measurement uncertainty – Part 3: Guide to the expression of uncertainty in measurement.

4.1.2 Measurement methodology

The Transient Plane Source (TPS) method employs a transient planar heat source for the rapid determination of thermal conductivity, thermal diffusivity, and consequently the specific heat capacity of a material. Among the main advantages of this technique, in addition to the possibility of testing a wide range of materials, is the large measurement range of thermal conductivity, which spans from 0.005 W/mK to 1800 W/mK.

The tests are non-destructive: an electric current flows through a nickel double-spiral sensor, generating a temperature increase in the system. The heat produced is dissipated into the sample on both sides of the sensor at a rate that depends on the thermal transport properties of the material. The sensor containing the nickel spiral therefore acts both as a heat source and as a temperature sensor.

via Duranti 93
06125 Perugia
Anna Pisello
Laura
075 585 3753
anna.pisello@unipg.it

By measuring the variation in the thermal resistance of the sensor during the thermal transient, the average temperature variation can be determined through the relation:

$$R(t) = R_0(1 + \alpha\overline{\Delta T(t)})$$

where R(t) is the electrical resistance [Ω] of the sensor at time t, R_0 is the initial resistance [Ω] of the sensor, α is the temperature coefficient of resistance, and ΔT(t) is the average temperature change [°C] of the sensor.

By analysing the temperature variation as a function of time, it is also possible to derive the thermal conductivity and thermal diffusivity of the surrounding material using the expression:

$$\Delta T(\tau) = \frac{P_0}{\pi^{\frac{3}{2}} r \lambda} D(\tau)$$

where P_0 is the power supplied by the sensor [W], r is the sensor radius [m], λ is the thermal conductivity [W/mK], and D(τ) is the dimensionless shape function defined as a function of the characteristic measurement time τ, and therefore of the thermal diffusivity k [mm²/s].

Finally, the specific heat capacity of the material can be obtained from the relation linking thermal conductivity and diffusivity:

$$k = \frac{\lambda}{\rho c_p}$$

The measurement methodology is based on the following assumptions:

- the planar sensor consists of concentric, equally spaced circular line sources;
- the thickness and heat capacity of the sensor are negligible;
- no thermal contact resistance is present between the sensor and the sample.

4.1.3 Experimental procedure

Thermal analyses were carried out using the Hot Disk instrument on samples with a diameter of 10 cm and a thickness of 2 cm. A Kapton 5501 sensor with a radius of 6.403 mm was placed between two halves of the same sample, ensuring full contact (Figure 10). For each sample, four

via Duranti 93 06125 Perugia Anna Laura Pisello 075 585 3753 anna.pisello@unipg.it

measurements were performed at four different locations. The mean value and standard deviation were then calculated.

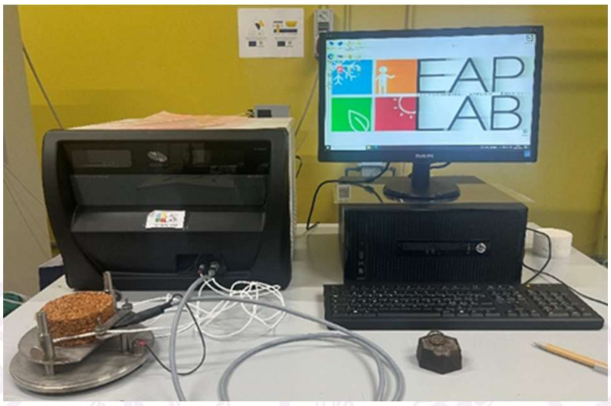

Figure 10. Experimental setup for thermal conductivity measurements using Hot Disk

4.1.4 Description of the instrumentation

Hot Disk TPS 2500 S

The Hot Disk instrument is designed for high-precision measurements of thermal transport properties such as thermal conductivity, thermal diffusivity, and specific heat capacity, using the hot disc method in accordance with ISO 22007-2. The device allows testing of a wide variety of materials with different geometries and dimensions.

The instrument available in the EAPLAB group is the Hot Disk AB – TPS 2500 S. The system mainly consists of a Wheatstone bridge and a flat sensor composed of a continuous double nickel spiral (thickness ≈ 10 µm), embedded between two Kapton layers with thickness between 0.013 and 0.025 mm. A DC power supply provides a constant voltage across the bridge, which is automatically balanced prior to each measurement. A digital voltmeter with memory records the temperature rise of the sensor and, consequently, the thermal transport properties of the investigated sample.

Thanks to multiple software modules, the instrument can be used for testing: (i) isotropic materials (Isotropic module), (ii) rod-shaped samples (One-dimensional module), (iii) thin films, coatings or adhesive layers (Thin-film module), (iv) conductive plates and slabs (Slab module), (v) extremely light and highly insulating materials (Low-density / Highly

via Duranti 93
06125 Perugia
Anna Pisello
Laura
075 585 3753
anna.pisello@unipg.it

insulating module), and (vi) anisotropic or layered materials (Anisotropic module). Moreover, since the device can probe thermal conductivity as a function of sample thickness (Structural probe module), it can also be used to assess material homogeneity.

During the test, the sensor is placed between two layers of the same material or between the sample and an insulating layer, and is heated by a constant electrical current. The heat generated inside the resistance dissipates into the surrounding material, producing a temperature rise of about 1–5°C, which is monitored through the resistance variation. The test duration is generally selected according to the sample thickness, in order to avoid heat losses to the surroundings. Furthermore, if the sample diameter is significantly larger than that of the sensor, the measurement area considered should be of the same order of magnitude as the sensor radius.

Table 8. Specifications of the Hot Disk TPS 2500 S instrument.

Thermal conductivity	0.005 ÷ 1800 W/m/K
Thermal diffusivity	0.1 ÷ 1200 mm^2/s
Volumetric specific heat	>5 MJ/m^3K
Measurement time	1 ÷ 1280 s
Repeatability	better than 1%
Accuracy	better than 5%
Temperature range	-253 ÷ 1000 °C
With circulator	-35 ÷ 200 °C
Minimum sample dimensions	• 0.5 × 2 mm diameter or area (mass test) • 0.1 × 10 mm diameter or area (slab test) • 10 × 5 mm diameter or area (unidirectional tests) • 0.02 × 22 mm diameter or area (thin-film tests)
Available sensor types	Kapton, mica o teflon

via Duranti 93
06125 Perugia
Anna Pisello
Laura
075 585 3753
anna.pisello@unipg.it

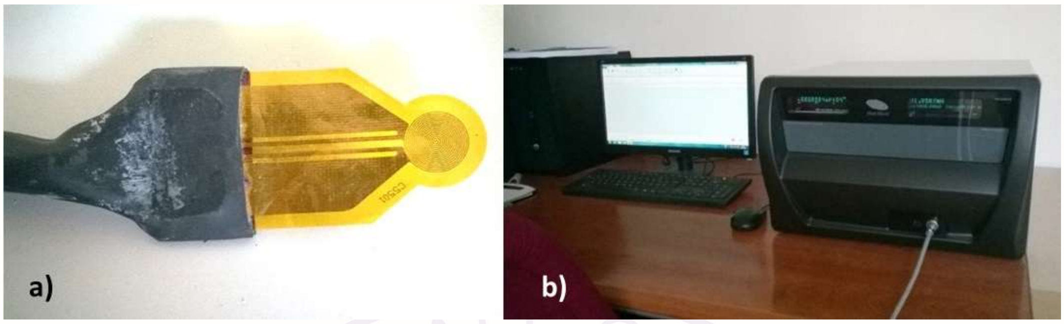

Figure 11. (a) Example of sensor and (b) Hot Disk TPS 2500 S, supplied to the EAPLAB laboratory (University of Perugia).

4.1.5 Results

In this section, the results of the thermal analyses performed on the four different types of samples are reported. For each sample, the thermal conductivity (λ), thermal diffusivity (D), and volumetric specific heat capacity (c) were evaluated.

Table 9. Results of thermal analyses before ageing.

Sample	Measure	λ [W/mK]	D [mm²/s]	c [MJ/m³K]
White	#1	1.66	1.07	1.6
	#2	1.63	1.26	1.3
	#3	1.63	1.28	1.3
	#4	1.69	1.12	1.5
	Average	1.65	1.2	1.4
	St.Dev.	0.03	0.1	0.1
Natural	#1	1.66	0.98	1.7
	#2	1.75	1.00	1.8
	#3	1.61	0.94	1.7
	#4	1.53	1.23	1.3
	Average	1.64	1.0	1.6
	St.Dev.	0.09	0.1	0.2
Red	#1	0.97	0.67	1.5
	#2	0.95	0.68	1.4
	#3	0.95	0.69	1.4
	#4	0.93	0.79	1.2
	Average	0.95	0.7	1.4
	St.Dev.	0.02	0.1	0.1
Black	#1	1.31	1.25	1.1
	#2	1.35	1.27	1.1
	#3	1.44	1.06	1.4
	#4	1.42	0.93	1.5
	Average	1.38	1.1	1.3
	St.Dev.	0.06	0.2	0.2

via Duranti 93
06125 Perugia
Anna Pisello
Laura
075 585 3753
anna.pisello@unipg.it

In particular, the white and natural samples exhibit very similar thermal properties, since they are made of the same materials except for the addition of white pigment. The red sample, produced using a different aggregate, shows the lowest thermal conductivity and thermal diffusivity among the four, while its volumetric heat capacity lies between that of the first two samples. The black sample, prepared using the same aggregate as the white and natural samples but with bitumen instead of the Evizero binder, shows slightly higher thermal properties than the red one. The change in binder may influence the thermal performance of the final material.

Figure 12 reports the thermal conductivity values of the samples after 30, 60, and 90 days of aging, whereas Table 10 reports the thermal diffusivity and volumetric heat capacity values. The results indicate that the aging process does not significantly affect the thermal properties of the materials, as the measured values remain comparable and consistent within the experimental uncertainty.

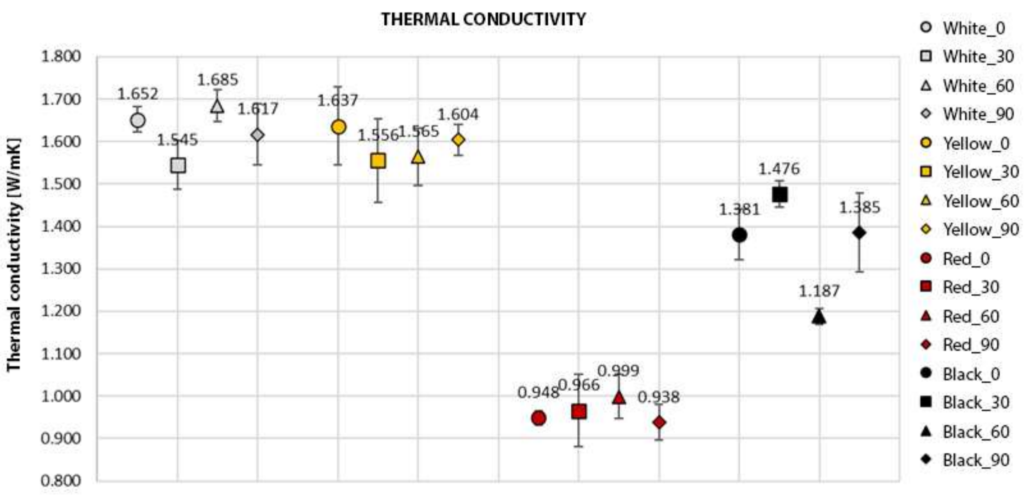

Figure 12. Thermal conductivity before and after the aging.

Ù

via Duranti 93
06125 Perugia
Anna Pisello
Laura
075 585 3753
anna.pisello@unipg.it

Table 10. Results of thermal analyses after aging.

Sample	Ageing time	Measure	D [mm²/s]	c [MJ/m³K]
White	30	**Average**	**1.1**	**1.4**
		St.Dev.	0.1	0.2
	60	**Average**	**1.0**	**1.9**
		St.Dev.	0.1	0.2
	90	**Average**	**1.3**	**1.4**
		St.Dev.	0.3	0.4
Natural	30	**Average**	**1.1**	**1.4**
		St.Dev.	0.1	0.2
	60	**Average**	**1.0**	**1.5**
		St.Dev.	0.1	0.2
	90	**Average**	**1.2**	**1.4**
		St.Dev.	0.1	0.1
Red	30	**Average**	**0.6**	**1.6**
		St.Dev.	0.1	0.2
	60	**Average**	**0.7**	**1.5**
		St.Dev.	0.1	0.2
	90	**Average**	**0.8**	**1.2**
		St.Dev.	0.1	0.2
Black	30	**Average**	**1.0**	**1.5**
		St.Dev.	0.1	0.2
	60	**Average**	**1.3**	**0.9**
		St.Dev.	0.2	0.1
	90	**Average**	**1.0**	**1.3**
		St.Dev.	0.1	0.1

via Duranti 93
06125 Perugia
Anna Pisello
Laura
075 585 3753
anna.pisello@unipg.it

5. Evaluation of Surface Overheating Performance, Air Temperature and Re-Emitted Radiation

5.1 Regulatory References

- D.P.R. 26/08/1993 n. 412
  Regulation containing provisions for the design, installation, operation and maintenance of building heating systems for the purpose of reducing energy consumption.

5.2 Measurement Methodology

To analyze the behavior of the samples under real environmental exposure conditions, a climate chamber was used in the EAPLAB laboratory at CIRIAF. The chamber is capable of accurately reproducing environmental parameters such as air temperature, relative humidity, and solar irradiance. The objective of this study is to evaluate the thermal behavior of the samples by simulating two representative summer days: an average summer day and an extreme hot summer day.

5.3 Test Procedure

For the thermal characterization tests, circular samples with a diameter of 15 cm and a thickness of 5 cm were used. Each sample was placed inside an insulating support made of 10-cm-thick polyurethane foam, leaving the upper surface of the sample directly exposed to the simulated environment inside the climatic chamber, while the lower surface remained in contact with the insulating support. A thermocouple was applied to both surfaces to record surface temperature values throughout the entire duration of the test.

The thermocouple positioned on the upper surface allows monitoring of the material response to direct exposure to the simulated environmental conditions, while the thermocouple on the lower surface enables evaluation of the heat flux through the sample. To complete the monitoring system, two TinyTag sensors for measuring air temperature and relative humidity (adequately shielded), and a pyranometer for measuring and recording solar irradiance, were installed inside the climatic chamber.

via Duranti 93 06125 Perugia Anna Pisello Laura 075 585 3753 anna.pisello@unipg.it

The described setup was used for both the average summer day and the hottest summer day. By analyzing the results of these tests, it is possible to evaluate how and to what extent each material heats up when exposed to specific environmental conditions, and therefore understand its thermal behavior.

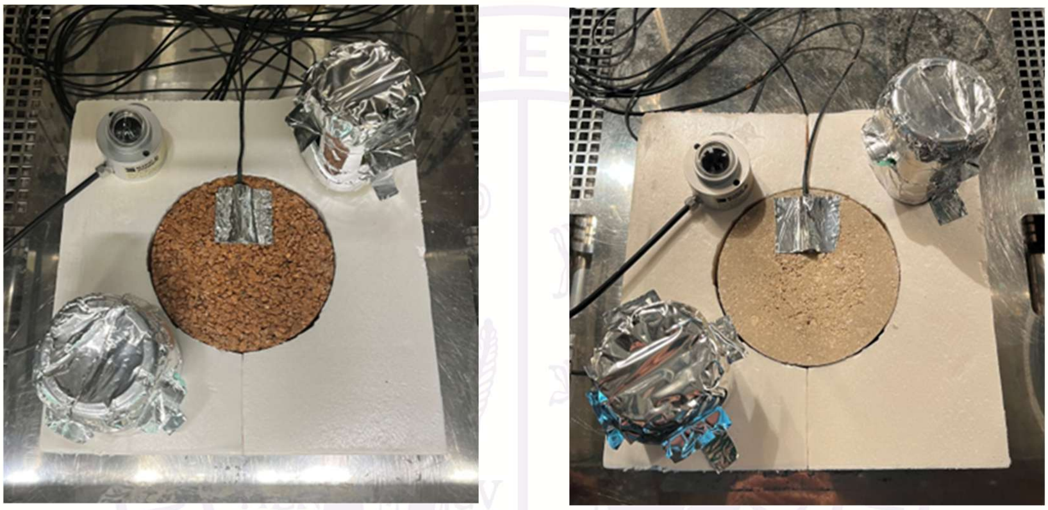

Figure 13. Experimental setup: sample inside the insulating base and related sensors.

5.3.1 Calculation of the Average Hourly Summer Day

The hourly parameters of the average summer day were calculated by averaging hourly data of temperature, relative humidity and solar radiation measured during 2023 at four different meteorological stations. The locations were selected to represent the climatic diversity of the Italian territory, making reference to the national climatic zoning system. This classification is based on heating degree-days, defined as the sum, over the year, of the difference between indoor design temperature and the average outdoor temperature: the higher the number of degree-days, the colder the climate (Table 11). In this analysis, the four reference climatic zones considered are: Zone B (Catania), Zone C (Bari), Zone D (Rome), and Zone E (Milan).

via Duranti 93 06125 Perugia Anna Laura Pisello 075 585 3753 anna.pisello@unipg.it

Table 11. Climate zones defined by Italian regulations and climate zones selected for the calculation of the average summer hourly day

Climatic zone	Degree Days
A	≤600
B	601 -900
C	901-1400
D	1401-2100
E	2101-3000
F	≥3001

Figure 14 shows the hourly average summer day derived from the meteorological data and used as reference for the climatic chamber simulations. Maximum solar irradiance approaches 800 W/m² during the central hours of the day, while maximum and minimum air temperatures are approximately 27 °C and 18 °C, respectively.

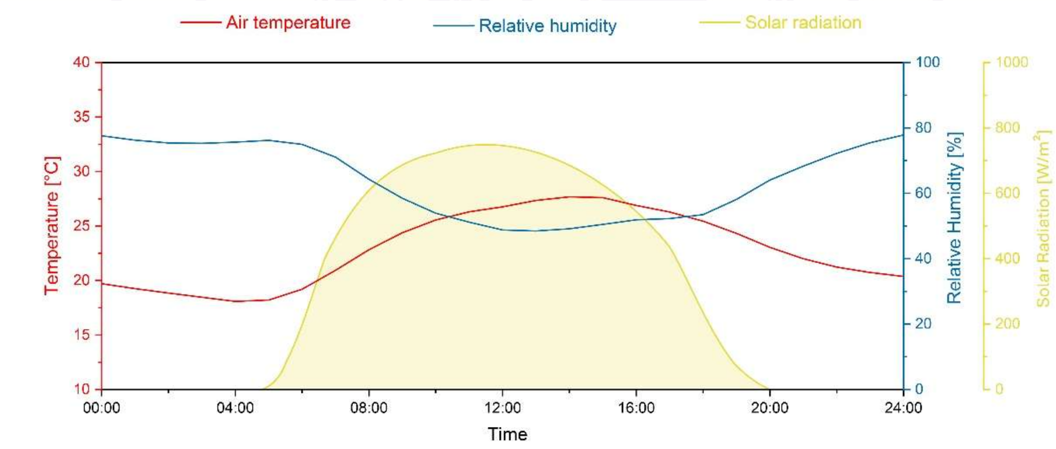

Figure 14. Temperature, relative humidity and irradiance profile during the calculated average summer hourly day.

5.3.2 Calculation of the Hottest Day

The day recording the highest air temperature in 2023 was identified from the meteorological data collected by the weather station located on the roof of the CIRIAF research centre building (Perugia, Italy). The selected day is 23/08/2023, and the corresponding environmental parameters are reported in Figure 15. Maximum solar irradiance approaches 1000 W/m² during midday hours, with peak air temperatures

via Duranti 93
06125 Perugia
Anna Pisello
Laura
075 585 3753
anna.pisello@unipg.it

exceeding 35 °C and minimum temperatures around 18 °C. Compared with the average summer day shown in Figure 14, the hottest day displays significantly lower relative humidity values, dropping below 15% during the central hours of the day.

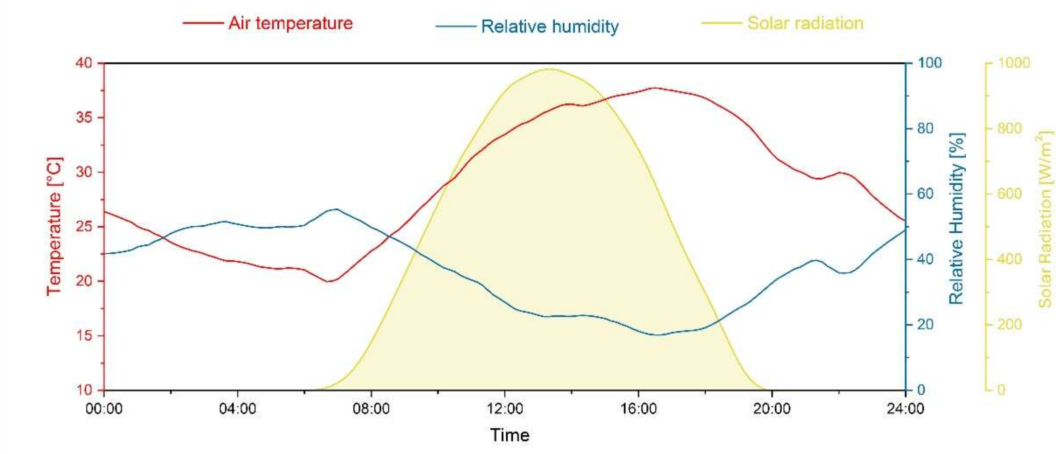

Figure 15. Temperature, relative humidity, and irradiance profile during the average summer hourly day obtained from the CIRIAF weather station.

5.3.3 Climatic Chamber Cycle Settings

The DM340SR climatic chamber at the EAPLAB laboratory is capable of simulating outdoor environmental conditions through precise control of air temperature, relative humidity and solar irradiance. The operating ranges of the chamber comfortably cover the air temperatures recorded during both the average and the hottest summer days of 2023, with humidity control down to 20%, to which any lower real values were approximated.

The solar simulator provides irradiance values between 600 and 1200 W/m², adequately reproducing the irradiance levels during the central daytime hours of the selected days. For irradiance values below 600 W/m², the solar-air temperature parameter (described in Section 5.3.4) was used, as it combines the thermal effects of solar radiation and air temperature. Since solar-air temperature depends proportionally on the optical properties of the material, a different irradiance-control profile had to be defined for each tested sample. Figure 16 shows the climatic-chamber settings used to reproduce the average hourly summer day, accounting for the different Italian climatic zones.

via Duranti 93
06125 Perugia
Anna Pisello
Laura
075 585 3753
anna.pisello@unipg.it

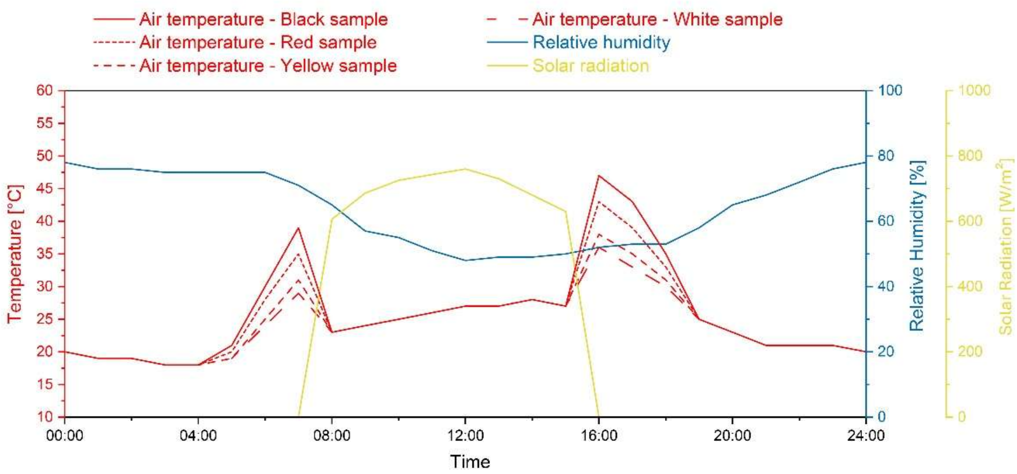

Figure 16. Settings used to simulate the average summer hourly day for each sample.

Figure 17 reports the settings used to reproduce the hottest day, as monitored by the CIRIAF weather station, for each tested sample.

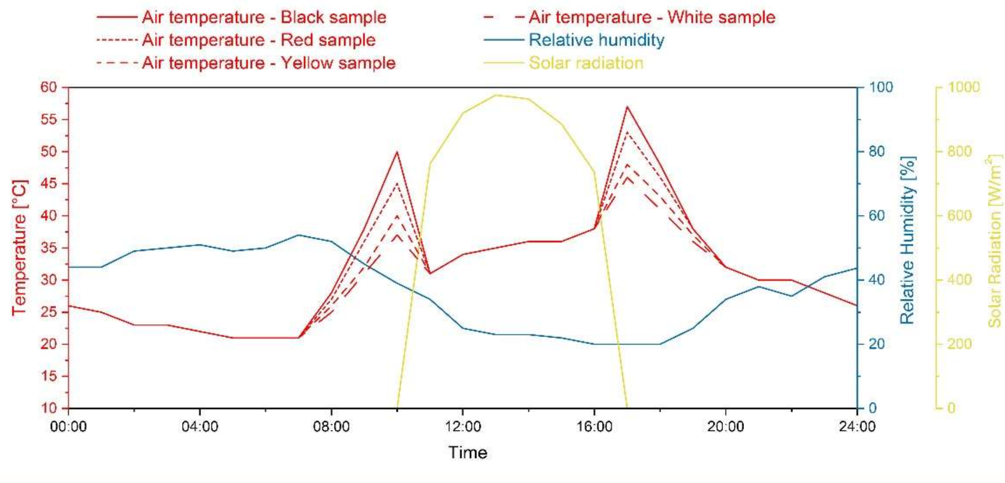

Figure 17. Settings used to simulate the hottest summer hourly day for each sample.

5.3.4 Solar-Air Temperature

The combined thermal effect of solar radiation and outdoor air temperature on an external surface is described by a single parameter: the solar-air temperature. This represents the fictitious outdoor air temperature that would cause, on a shaded surface, the same heat exchange as that generated in reality by the combined action of outdoor temperature and solar radiation.

via Duranti 93
06125 Perugia
Anna Laura Pisello
075 585 3753
anna.pisello@unipg.it

The sun-air temperature is calculated from the following relation:

$$T_{sun-air} = T_{ext} + \frac{(\alpha \cdot I_{total})}{h_0} - \frac{(\varepsilon \cdot \Delta R)}{h_0}$$

where:

- T_{ext} outdoor air temperature at the surface;
- α solar absorptance of the surface;
- I_{total} incident solar irradiance;
- h_0 external heat transfer coefficient;
- ε thermal emissivity;
- ΔR net radiant exchange term.

For horizontal surfaces such as pavements, $(\varepsilon \cdot \Delta R)/h_0$ can be considered equal to zero. The previous expression therefore becomes:

$$T_{sun-air} = T_{ext} + \frac{(\alpha \cdot I_{total})}{h_0}$$

From this equation, it is evident that the solar-air temperature is directly proportional to the optical properties of the external surface finishing. Therefore, under identical climatic conditions, a dark surface with high solar absorptance will exhibit a higher solar-air temperature than a light-colored one, and consequently a higher heat flux towards the indoor environment.

5.3.5 Calculation of Average Re-Emitted Radiation

The calculation of the radiation emitted by a sample is essential to understanding the surface energy balance and, consequently, its thermal behavior. In particular, for materials used outdoors, the ability of a surface to emit or retain heat directly affects several aspects, including thermal comfort optimization and the potential mitigation of the urban heat island effect.

via Duranti 93 06125 Perugia Anna Pisello Laura 075 585 3753 anna.pisello@unipg.it

The Stefan–Boltzmann law describes the total radiant power emitted by a surface as a function of its temperature. This law is fundamental for calculating thermal losses or gains through radiation and is used to assess the thermal behavior of materials and surfaces exposed to different environmental conditions. Specifically, it is expressed as:

$$P_e = \varepsilon \cdot \sigma \cdot T^4$$

where:

- P_e emitted power per unit area (W/m^2);
- ε surface emissivity;
- σ Stefan-Boltzmann constant (5.67x10^{-8} W/m^{2}K^4);
- T absolute surface temperature (K).

In addition to calculating the total radiation emitted by the sample, the calculation of the net emitted radiation is equally important, as it indicates the amount of heat effectively dissipated by the surface to its surroundings. This calculation makes it possible to determine the actual heat exchange between the sample and the sky through net radiative emission. In this case, the equation can be rewritten as follows:

$$P_e = \varepsilon \cdot \sigma \cdot (T_{surface}^4 - T_{sky}^4)$$

dove:

- P_e emitted power per unit area (W/m^2);
- ε surface emissivity;
- σ Stefan-Boltzmann constant (5.67x10^{-8} W/m^{2}K^4);
- $T_{surface}$ absolute surface temperature (K);
- T_{sky} sky temperature, assumed equal to air temperature minus 10 K (K).

In this analysis, both total and net emitted radiation were calculated over a two-hour time window corresponding to the highest recorded temperatures for the average summer day and the hottest day. Surface and air temperature data within this interval were averaged to obtain a single representative value to be used in the radiation emission calculations.

via Duranti 93
06125 Perugia
Anna Laura Pisello
075 585 3753
anna.pisello@unipg.it

5.4 Description of the Instrumentation Used

<u>Climatic Chamber DM340SR</u>

A climatic chamber is equipment that allows environmental conditions to be artificially reproduced, in order to assess the effects on machinery, materials, devices, or electronic components. The unit available at the EAPLAB laboratory at CIRIAF, University of Perugia, is the DM340SR model manufactured by Angelantoni Test Technologies (ATT). It features a test chamber in which a controlled environment can be obtained in terms of temperature, relative humidity, and solar radiation, the latter simulated using a halogen lamp with a solar spectrum representative of typical mid-latitude conditions. The inner chamber is constructed from stainless steel sheet (AISI 304), fully welded to ensure vapor tightness. Thermal insulation is provided by glass wool treated with a special thermosetting resin binder.

The operation of the climatic chamber is ensured by three systems: (i) heating, (ii) cooling, and (iii) dehumidification. The heating system consists of stainless-steel sheathed electric resistances with low thermal inertia, placed along the internal air recirculation path. The cooling system uses ozone-safe refrigerants, and cooling is produced by the evaporation of the liquid injected into the evaporator. The compressor pressurizes the refrigerant gas in the condenser, where, due to the high pressure, it condenses into liquid form. The liquid refrigerant is then expanded through a thermostatic valve and evaporates, absorbing heat and thus cooling the test chamber. The cycle is completed when the gas is sucked back into the compressor.

The dehumidification system operates using the "cold finger" technology. A small smooth-tube evaporator, powered by the same cooling unit, freezes the moisture in the air in contact with it, without affecting the chamber temperature. Humidification is achieved through direct injection of steam into the chamber. The direct humidification system uses a special steam generator that delivers superheated water vapor, eliminating the risk of dripping. This direct system has a very rapid response time, enabling fast changes in humidity. The entire process is controlled by a regulator that accounts for the nonlinear dependence between air temperature and moisture content.

via Duranti 93 06125 Perugia Anna Pisello Laura 075 585 3753 anna.pisello@unipg.it

Table 12. Specifications of teh climatic chamber ATT UD150C SR.

Useful volume	337 l
Temperature range	-40 ÷ +180 °C
Accuracy (over time and at the center of the working space)	±0.5-1.0 °C
Humidity range	10÷98%
Relative humidity range	±1÷3 %
Continuous dew point operating range	-4/+94 °C
Non-continuous dew point operating range	-3/+4 °C
Maximum thermal load at +25 °C	2300 W
Refrigerant gas	R404A
External dimensions	919x1786x1765 mm
Internal working dimensions	601x810x694 mm
Maximum load capacity	80 Kg
Total machine weight	820 Kg
Airborne noise level with air-cooled condenser	58 dB

Figure 18. Climatic chamber ATT DM340SR, available at EAPLAB@CIRIAF (Università degli Studi di Perugia).

via Duranti 93 06125 Perugia Anna Pisello Laura 075 585 3753 anna.pisello@unipg.it

FLIR Thermal Camera

A thermal camera is a device that detects heat emitted by objects, people, or surfaces in the form of infrared radiation. This radiation is invisible to the human eye but is emitted by all bodies with a temperature above absolute zero (−273.15 °C). The thermal camera converts this radiation into a visible image, known as a thermal image, which displays temperature differences through colors or tonal gradients.

In this analysis, a compact FLIR One thermal camera was used to acquire infrared thermal images of the samples during the climatic chamber simulations. The FLIR One combines thermal images with visible-light images using MSX (Multi-Spectral Dynamic Imaging) technology, which overlays visual details onto the thermal image to improve clarity and readability.

Table 13. Specifications of FLIR One thermal camera.

Dimensions	35 × 37.5 × 149 mm
Weight	153 g
Thermal pixel size	12 µm
Thermal resolution	160 × 120 (19.200 pixel)
Thermal sensitivity	70 m
Object temperature range	-20°C a 120°C
Operating temperature	-10°C a 50°C
Accuracy	±3°C

TinyTag

The Tinytag Plus 2 TGP-4017 is a data logger designed to monitor both temperature and relative humidity. Thanks to its internal sensors, it is capable of detecting temperatures between −25 °C and +85 °C and relative humidity levels between 0% and 100%, making it suitable for a wide range of applications. With a memory capacity of up to 32,000 readings, this device enables continuous long-term monitoring while ensuring accuracy and reliability even under extreme conditions. Its robust waterproof housing protects it from external agents, allowing use without compromising the integrity of the collected data. Power is

via Duranti 93
06125 Perugia
Anna Laura Pisello
075 585 3753
anna.pisello@unipg.it

supplied by a replaceable battery with an average life of approximately 2 years, depending on the logging frequency.

Table 14 – Specifications of TinyTag sensors.

Dimensions	34 × 51 × 80 mm
Weight	110 g
Reading resolution	0.01 °C
Reading types	Actual, Minimum, Maximum
Operating range	-40°C to +85°C
Logging interval	1 second to 10 days
Sensor type	NTC 10K thermistor
Protection rating	IP68 waterproof
Total memory capacity	32.000 readings

5.5 Results

This section presents the results of the thermal monitoring of the samples when subjected to specific environmental conditions in the climatic chamber, simulating in particular an average summer day and an extremely hot summer day.

5.5.1 Results of the Simulation of the Average Hourly Summer Day

Figures 19-22 show the surface temperature profiles of the different samples during the climatic chamber simulation. Consistent with their solar radiation absorption capability and with the previously calculated SRI values, the White and Natural samples exhibit the lowest surface temperatures on the exposed side, with maximum values of 44 °C and 48 °C, respectively. On the unexposed lower surfaces, temperatures are approximately 2 °C lower.

For the Red sample, the difference between exposed and unexposed surfaces is more pronounced (around 3 °C), with the maximum exposed-surface temperature exceeding 51 °C. The Black sample shows the poorest performance in terms of overheating, reaching peak temperatures of 55 °C on the exposed surface and 51 °C on the unexposed surface. In all cases, the air temperature trend (dashed blue line) varies significantly when the solar-air temperature is considered, showing two main peaks in

via Duranti 93
06125 Perugia
Anna Laura Pisello
075 585 3753
anna.pisello@unipg.it

the early morning and late afternoon, directly related to the solar absorptance of each sample.

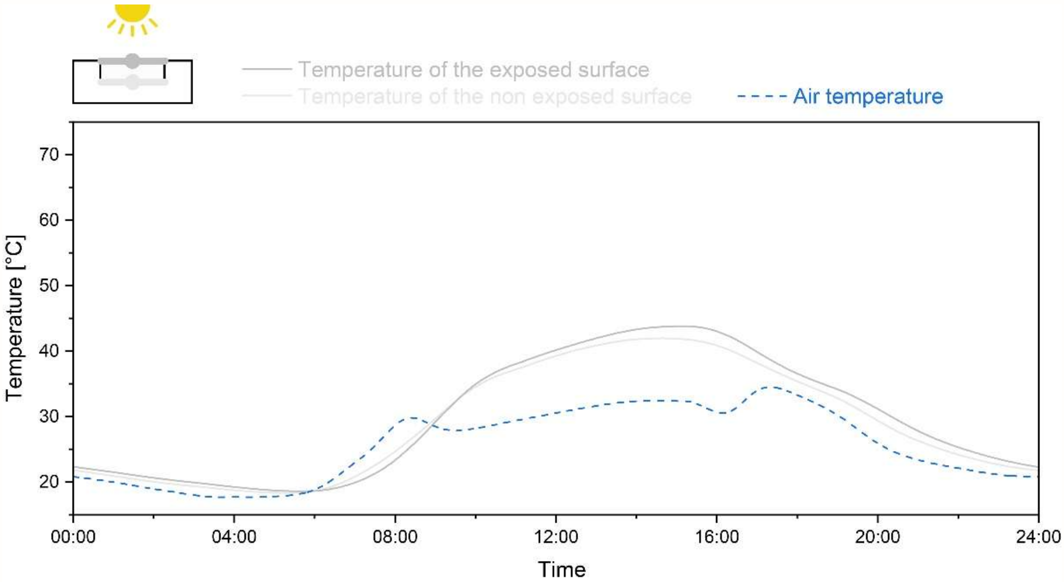

Figure 19. Simulation results for the average summer hourly day – White Sample.

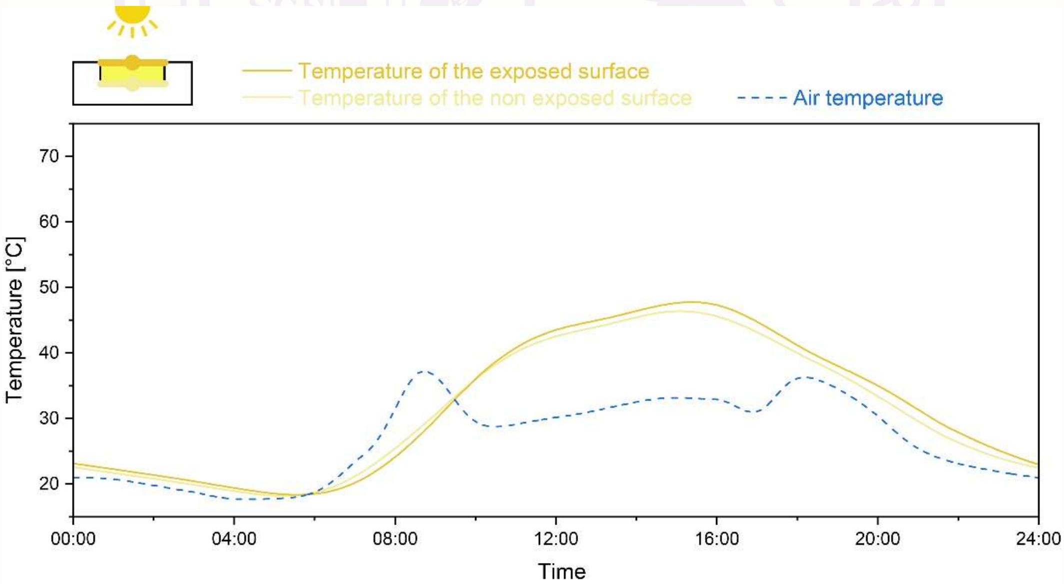

Figure 20. Simulation results for the average summer hourly day – Natural Sample.

via Duranti 93
06125 Perugia
Anna Pisello
Laura
075 585 3753
anna.pisello@unipg.it

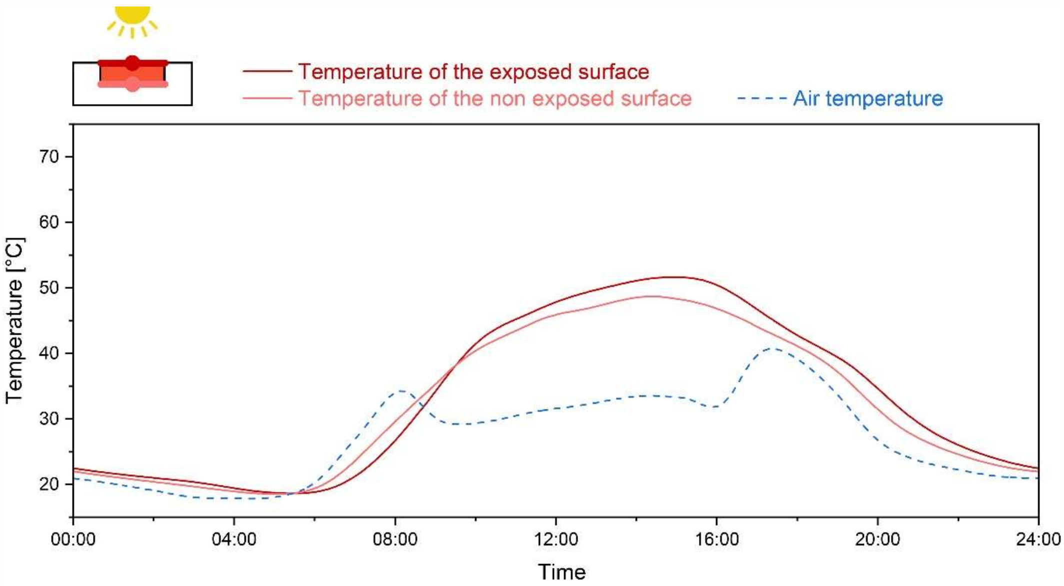

Figure 21. Simulation results for the average summer hourly day – Red Sample.

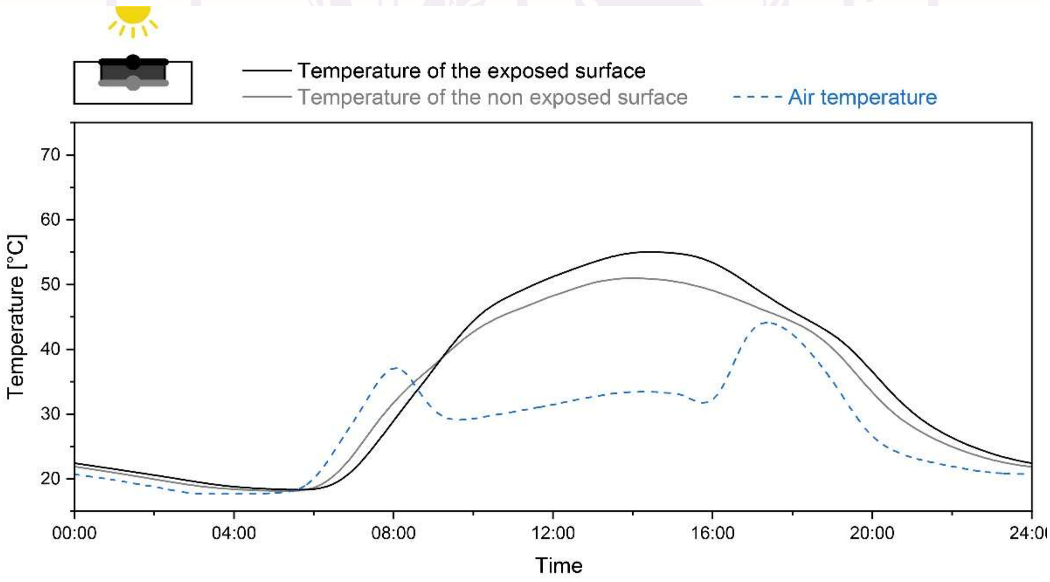

Figure 22. Simulation results for the average summer hourly day –Black Sample.

During the hottest hours of the simulated average summer day, thermographic images were also taken for each sample, as shown in Figure 23. The thermographic images show surface temperatures

via Duranti 93
06125 Perugia
Anna Pisello
Laura
075 585 3753
anna.pisello@unipg.it

consistent with the data obtained from surface temperature monitoring using temperature probes.

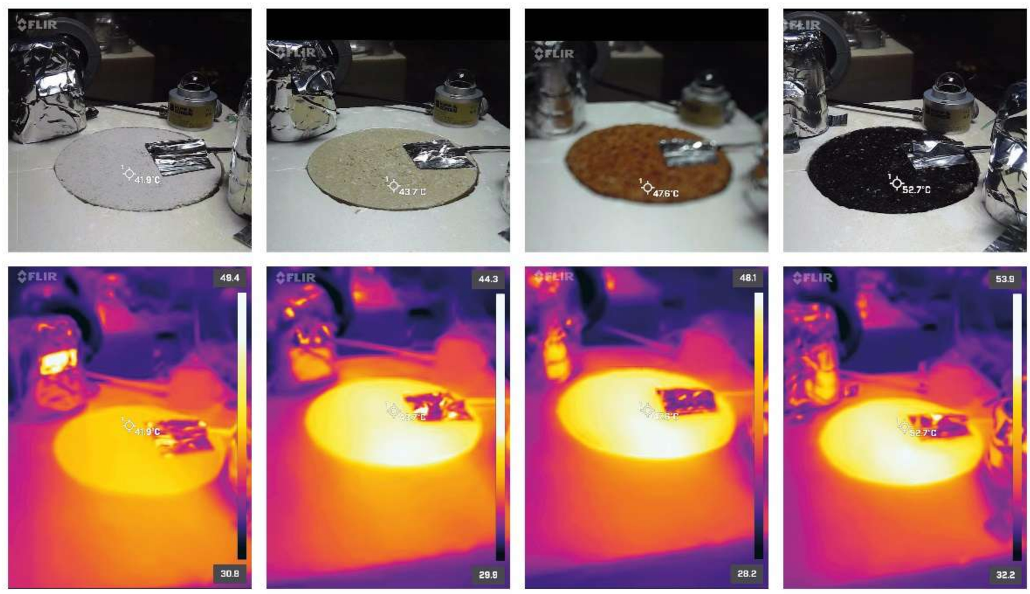

Figure 23. Thermographs acquired during the simulated average summer day.

5.5.2 Results of the Simulation of the Hottest Summer Day

Figures 24-27 show the surface temperature profiles of the different samples during the climatic chamber simulation of the hottest summer day. As in the case of the average day, the White and Natural samples exhibit the lowest exposed-surface temperatures, with maximum values of 55 °C and 59 °C, respectively. On the unexposed surfaces, temperatures remain approximately 2 °C lower. For the Red sample, the difference between exposed and unexposed surfaces is again more marked (up to 4 °C), with the exposed surface temperature exceeding 67 °C. The Black sample again shows the poorest performance in terms of overheating, reaching maximum values of 70 °C on the exposed surface and 65 °C on the unexposed surface. Also in this case, the air temperature trend is influenced by the solar-air temperature settings, showing two peaks in the early morning and late afternoon.

via Duranti 93
06125 Perugia
Anna Laura Pisello
075 585 3753
anna.pisello@unipg.it

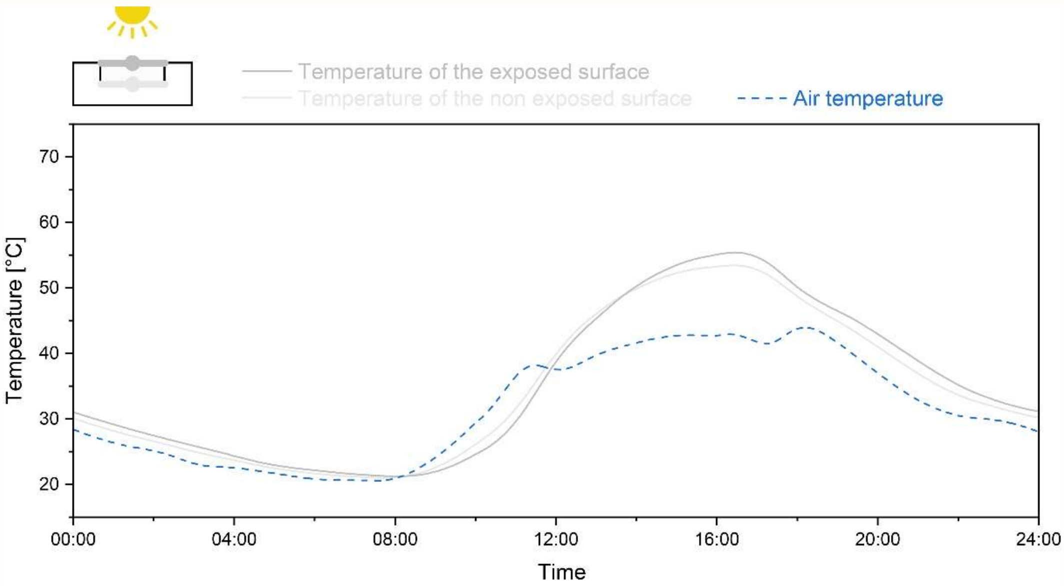

Figure 24. Simulation results for the hottest summer hourly day –White Sample.

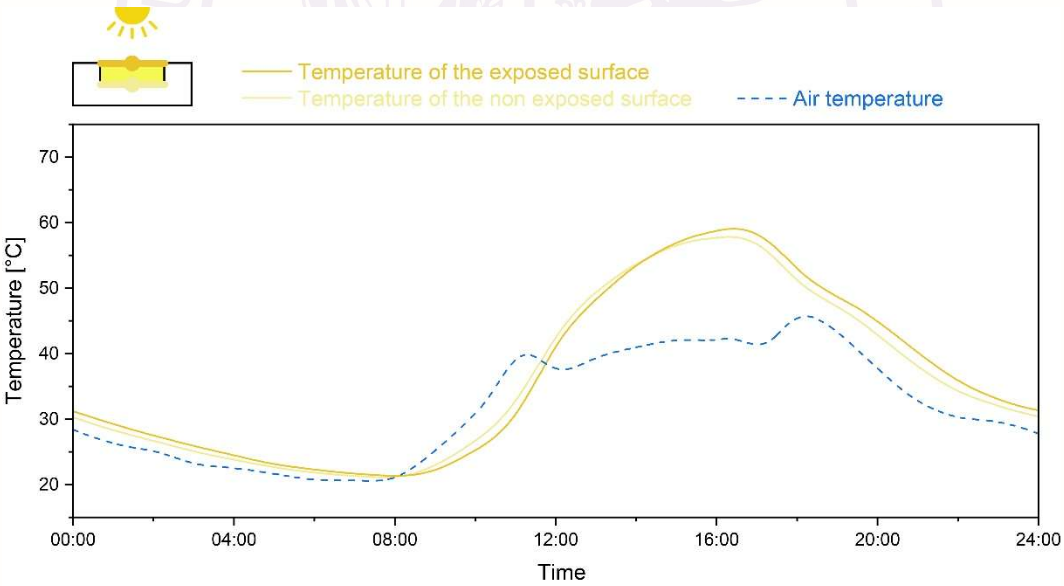

Figure 25. Simulation results for the hottest summer hourly day –Natural Sample.

via Duranti 93
06125 Perugia
Anna
Pisello
Laura
075 585 3753
anna.pisello@unipg.it

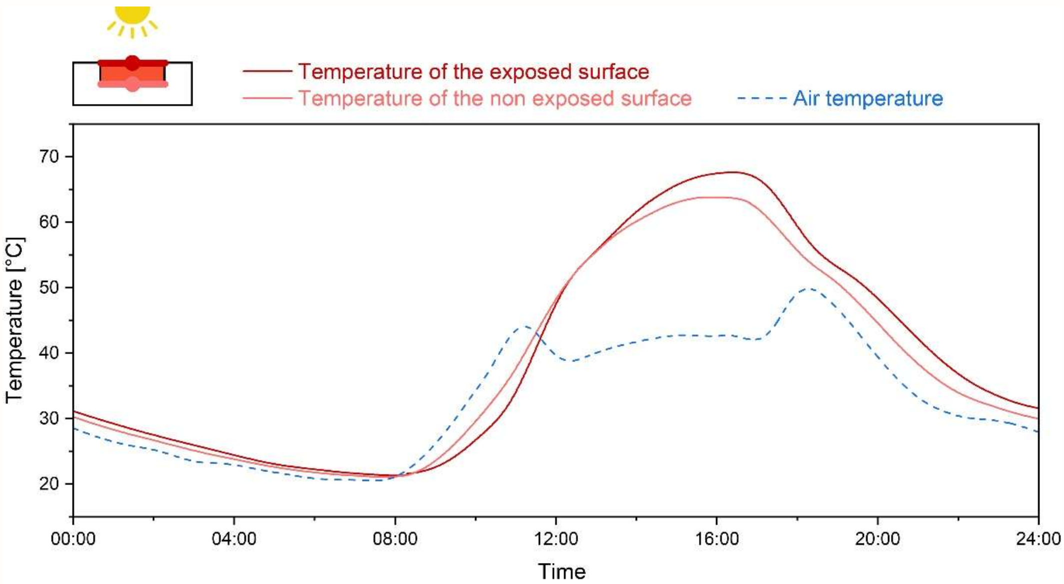

Figure 26. Simulation results for the hottest summer hourly day –Red Sample.

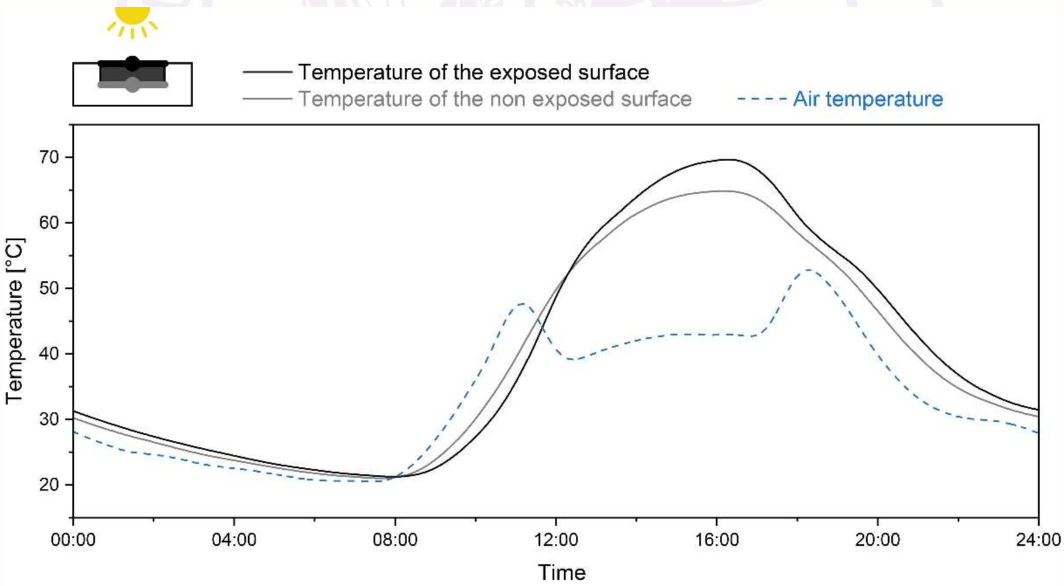

Figure 27. Simulation results for the hottest summer hourly day –Black Sample.

During the hottest hours of the simulated average summer day, infrared thermographic images were also taken for each sample, as shown in Figure 28. As in the previous case, the thermographic images indicate surface temperatures consistent with those recorded by the temperature probes during thermal monitoring.

via Duranti 93 06125 Perugia
Anna Pisello
Laura
075 585 3753
anna.pisello@unipg.it

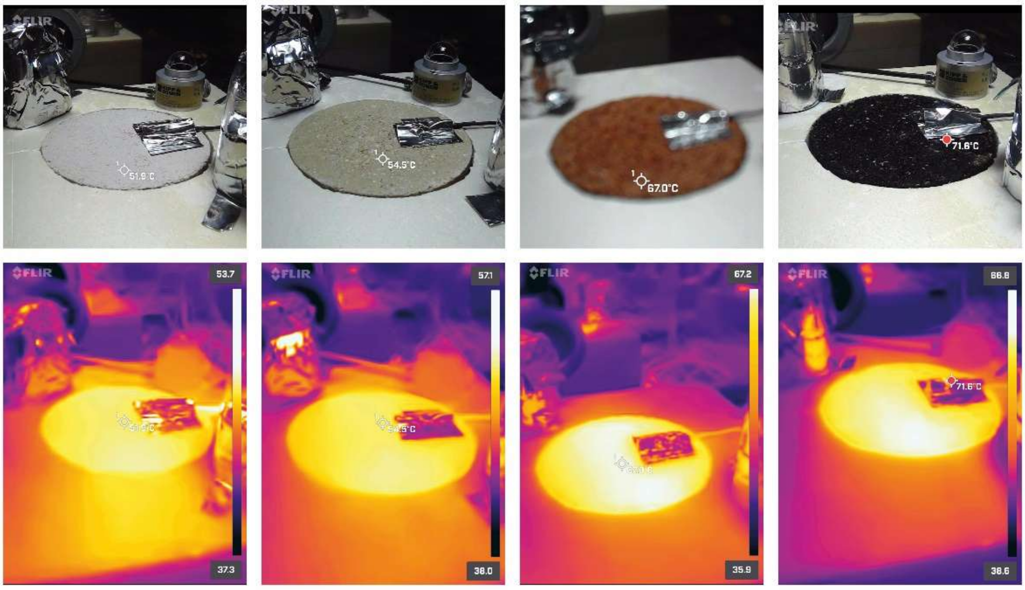

Figure 28. Thermographs acquired during the simulated hottest summer day.

5.5.3 Comparison between samples

Figures 29–30 compare the thermal performance of the samples during the climatic chamber simulations in terms of temperature differences on the surfaces directly exposed to solar radiation. From the analysis of the average days, the Black sample shows the highest temperatures, reaching 55.0 °C on the exposed surface. Compared to these values, the White sample remains cooler by approximately 11 °C. The Red sample shows temperatures about 3 °C lower than the Black one, while the Natural sample is about 7 °C cooler.

On the hottest simulated summer days, the same trend is confirmed, with the Black sample again reaching the highest values: 69.7 °C on the surface exposed to solar radiation. In this case, the White sample remains cooler by about 14 °C, the Natural sample shows temperatures approximately 11 °C lower, while the Red sample is only slightly cooler than the Black one, with differences of about 2 °C. Overall, the data confirm that color tone strongly influences overheating, with lighter samples ensuring significant reductions in surface temperature compared to darker ones.

via Duranti 93
06125 Perugia
Anna Laura Pisello
075 585 3753
anna.pisello@unipg.it

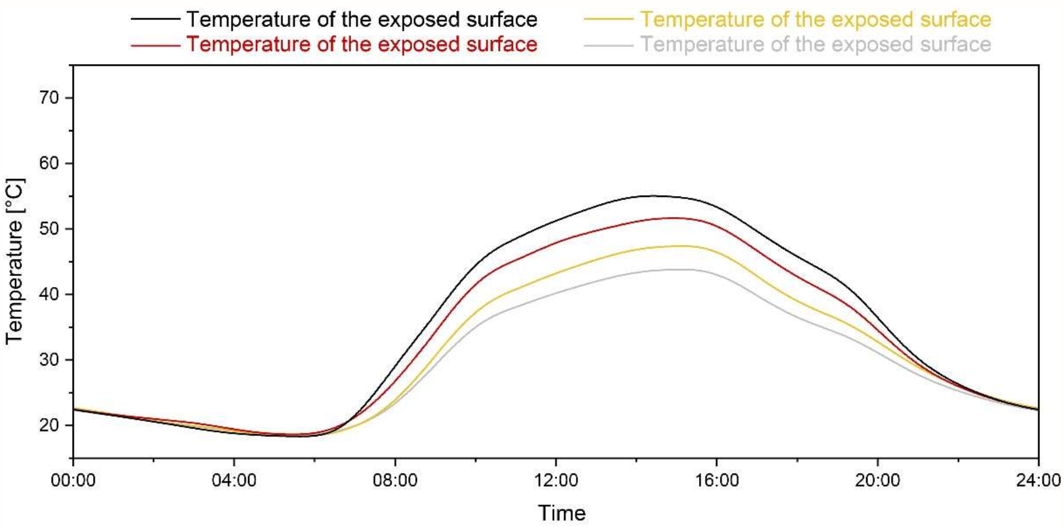

Figure 29. Comparison between samples – Average summer hourly day.

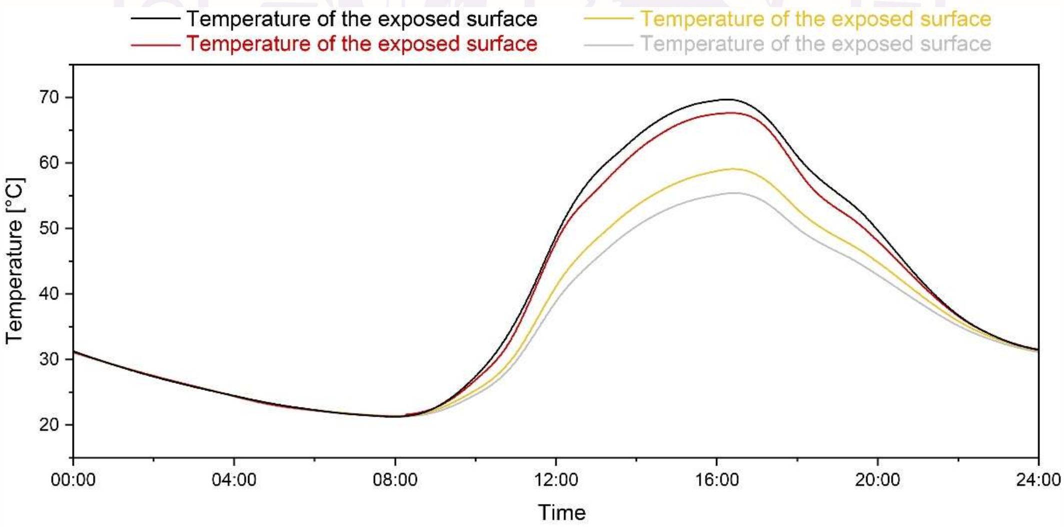

Figure 30. Comparison between samples – Hottest summer hourly day.

Table 15 reports the results relating to thermal radiation emitted by the four analyzed samples. In both simulated days, the total emitted radiation increases with increasing darkness of the sample: the black sample shows the highest values, followed by red, natural and finally white. This trend is due to the greater overheating of darker surfaces, since the thermal radiation emitted by a body is directly proportional to its surface temperature.

via Duranti 93
06125 Perugia
Anna Pisello
Laura
075 585 3753
anna.pisello@unipg.it

Table 15 – Calculation of the emitted radiation

Sample	Simulated day	Total emitted radiation (W/m^2)
White	average	536
	hottest	604
Natural	average	556
	hottest	623
Red	average	603
	hottest	714
Black	average	628
	hottest	733

via Duranti 93
06125 Perugia
Anna Laura Pisello
075 585 3753
anna.pisello@unipg.it

6. On-site monitoring of surface temperature, near-surface air temperature, and albedo

6.1 Regulatory references

- ISO 9060:2018
  Solar energy — Specification and classification of instruments for measuring hemispherical and direct solar radiation
- ISO 9846:2025
  Solar energy — Calibration of a pyranometer using a pyrheliometer
- ISO 9847:2023
  Solar energy — Calibration of field pyranometers by comparison to a reference pyranometer
- ISO/TR 9901:2021
  Solar energy — Pyranometers — Practical recommendations for use

6.2 Measurement methodology

The instrument used for this type of analysis is the Hukseflux Thermal Sensors NR01 4-component radiometer. This instrument is a 4-component net radiometer that provides measurements of global solar radiation, reflected solar radiation, and downward and upward longwave radiation, using two upward-facing and two downward-facing sensors capable of detecting shortwave (solar) and longwave (thermal) radiation respectively. NR01 is therefore able to measure the four components separately: solar radiation and upward and downward longwave radiation. To do so, it uses pyranometers (solar radiation sensors) and pyrgeometers (longwave radiation sensors). By analyzing these four components, the net radiation can be determined, while calculation of sky and surface temperature requires compensation for the heat emitted by the pyrgeometers themselves (Stefan–Boltzmann law).

The NR01 is therefore also equipped with a PT100 temperature sensor, a pyranometer model SR01 for monitoring solar irradiance, a second equivalent sensor for monitoring radiation reflected by the pavement under analysis, two pyrgeometers model IR01 for longwave radiation analysis, and an internal heating system to prevent condensation, particularly during nighttime.

via Duranti 93
06125 Perugia
Anna Laura Pisello
075 585 3753
anna.pisello@unipg.it

Solar irradiance measured in W/m² is calculated by dividing the SR01 output, a small voltage signal, by the sensitivity value stated on the SR01 calibration certificate. The equation governing solar radiation measurement is:

$$E = \frac{U}{S}$$

where U is the output voltage (V) and S is the sensitivity (V/(W/m²)).

Longwave irradiance in W/m² is instead calculated by dividing the IR01 output voltage U by the sensitivity S and accounting for the heat emitted by the sensor itself (Stefan–Boltzmann law). The sensitivity is specified on the IR01 calibration certificate. The equation governing longwave radiation measurement with the pyrgeometers is the following:

$$E = \frac{U}{S} + \sigma \cdot (T + 273.15)^4$$

From the upward and downward solar radiation components, it is possible to calculate the net solar radiation and albedo or surface reflectance. From all four shortwave and longwave components, the net radiation and surface temperature can be derived.

Figure 31 shows the NR01 4-component net radiometer used for the analysis of shortwave solar radiation.

Figure 31. NR01 4-component net radiometer (pyrgeometers on the left and pyranometers on the right of the image).

The equations considered in this analysis are as follows:

- For the upward- and downward-facing pyranometers, measuring global solar radiation E_g and reflected solar radiation E_r:

via Duranti 93 06125 Perugia Anna Pisello Laura 075 585 3753 anna.pisello@unipg.it

$$E_g \downarrow_h = \frac{U}{S}$$
$$E_r \uparrow = \frac{U}{S}$$

- Net radiation and albedo (in the calculation of net radiation, the instrument temperature is no longer included):

$$E^* = E\downarrow - E\uparrow = E_g\downarrow_h - E_r\uparrow + E_l\downarrow - E_l\uparrow$$

$$Albedo = \frac{E_r\uparrow}{E_g\downarrow_h}$$

6.3 Test procedure

For the analysis of on-site monitoring of surface temperature, near-surface air temperature (50 cm), and albedo, the 4-component sensor was installed over a test pavement specifically constructed as a measurement field by the company PAV.I. Srl in Moano (06034, Foligno (PG)). For the construction of this test field, a slightly different aggregate was used, although still a light-coloured limestone similar to the "Bianco Ancona" aggregate (Figure 32).

a)  b)

Figure 32. a) Test field, b) focus on the pavement.

The surface was monitored over a period of three days, from 25 to 27 June 2025. For this purpose, the 4-component sensor was positioned

via Duranti 93 06125 Perugia Anna Pisello Laura 075 585 3753 anna.pisello@unipg.it

parallel to the pavement surface, in a central location but sufficiently distant from shaded areas produced by nearby vegetation, in order to avoid any alteration of the measured data.

In addition, TinyTag sensors were used to measure pavement surface temperature, air temperature, and relative humidity (at 50 cm height) for the entire monitoring period. Once installed as shown in Figure 33, the sensor was connected to the data logger to record the monitored parameters with an acquisition interval of 30 seconds.

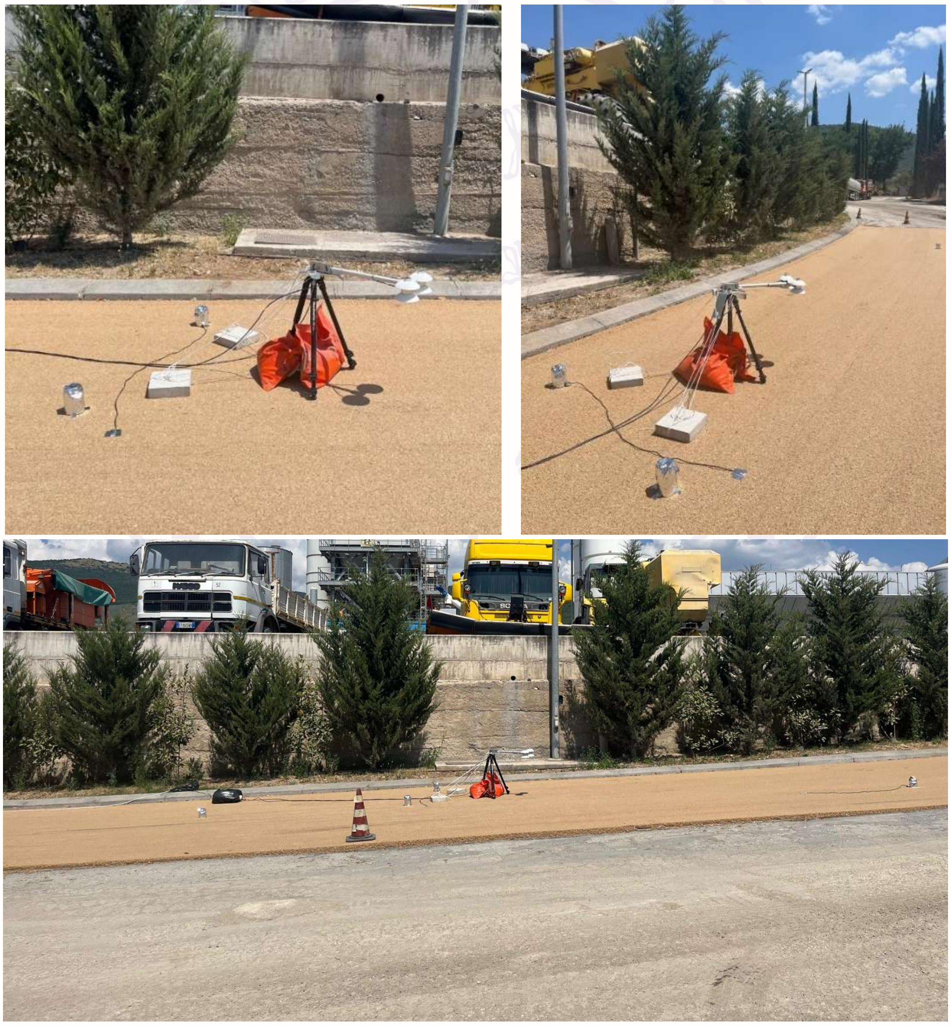

Figure 33. Test field during the monitoring campaign.

via Duranti 93
06125 Perugia
Anna Laura Pisello
075 585 3753
anna.pisello@unipg.it

6.4 Description of the instruments used

The NR01 sensor is a 4-component net radiometer consisting of two SR01 pyranometers (used in this study for solar radiation analysis), two IR01 pyrgeometers, a heater, a levelling device for the x and y axes, and a PT100 temperature sensor. Table 16 lists the technical details and specifications of the sensor.

Table 16. Specifications of NR01 sensor.

Included sensors	2 Second Class ISO 9060 pyranometers 2 pyrgeometers with a 150° field of view
Solar spectral range	From 285 to 3000 x 10^{-9} m
Longwave spectral range	From 4.5 to 40 x 10^{-6} m
Leveling	Bubble level and x-y leveling assembly included
Sensor power requirement	Zero (passive sensor)
Temperature sensor	Pt100
Pyrgeometer heater	12 VDC, 1.5 W
Nominal operating temperature range	From -40 to +80 °C
Nominal operating relative humidity range	From 0 to 100%
Required data acquisition inputs	4 differential voltage channels or single-ended voltage channels, input resistance > 10^6 Ω 1 temperature channel for Pt100
Standars governing instrument use	ISO/TR 9901:1990 Solar energy - Field pyranometers - Recommended practice for use ASTM G183 - 05 Standard Practice for Field Use of Pyranometers, Pyrheliometers and UV Radiometers
ADDITIONAL SPECIFICATIONS - SR01 PYRANOMETER	
Measurement	Gloval and reflected solar radiation Irradiance W/m^2
Field of view	180°
Measurement range	From 0 to 2000 W/m^2
Sensitivity range	From 7 to 30 x 10^{-6} V/(W/m^2)
Nominal sensitivity	15 x 10^{-6} V/(W/m^2)

via Duranti 93 06125 Perugia Anna Pisello Laura 075 585 3753 anna.pisello@unipg.it

Expexted output voltage	For applications under natural solar radiation: from –0.1 to +50 x 10^{-3} V
Required measurement / programming function	E=U/S
Sensor resistance range	From 40 to 60 Ω
Sensor power requirement	Zero (passive sensor)
Spectral range (20% transmission points)	From 285 to 3000 x 10^{-9} m

6.5 Results

This section reports the results of the on-site monitoring carried out on the Evizero pavement over three days. Specifically, incoming (IN) and outgoing (OUT) shortwave and longwave solar radiation were monitored in W/m², together with net shortwave and longwave radiation, obtained as the difference between incoming and outgoing radiation. Surface temperature (°C), albedo, air temperature, humidity, and surface temperature were also measured using TinyTag sensors.

Figure 34 shows the trend of the monitored temperature over the entire experimental campaign. From the recorded temperature data, it can be observed that the test was conducted on characteristically hot days, with peak temperatures around 40 °C during the central hours of the day, decreasing to approximately 20 °C during the night.

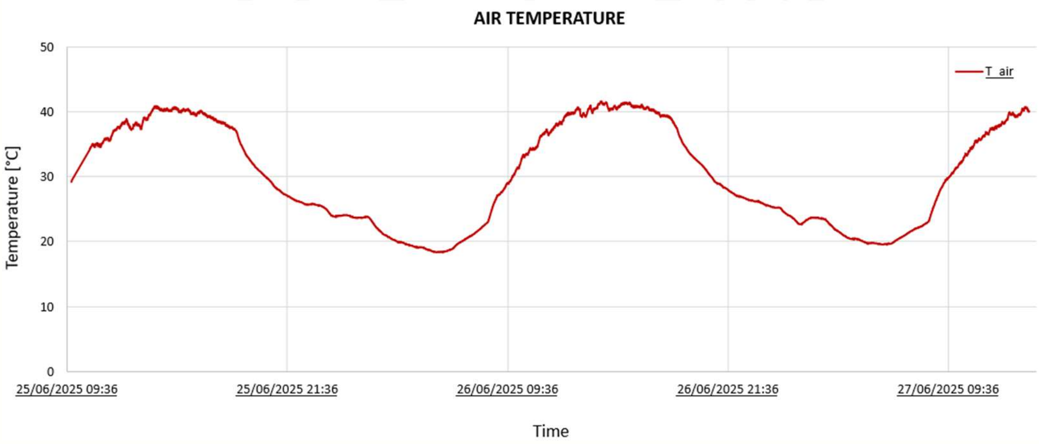

Figure 34. Measured air temperature.

via Duranti 93
06125 Perugia
Anna Laura Pisello
075 585 3753
anna.pisello@unipg.it

Figure 35 shows a typical daily trend of solar radiation during the monitoring period. The incoming component (SW_IN) reaches its maximum around 1:00 p.m., with peaks of approximately 940 W/m² at 13:34 on 25 June and at 13:33 on 26 June, while the day of 27 June shows slightly lower solar radiation values. The outgoing solar radiation (SW_OUT), i.e., the component reflected from the analyzed surface, reaches values slightly below 300 W/m² during the hottest hours. The net solar radiation (SW_NET) is given by the difference between IN and OUT and reaches approximately 650 W/m² during the central hours of the day, which is consistent with clear-sky summer conditions.

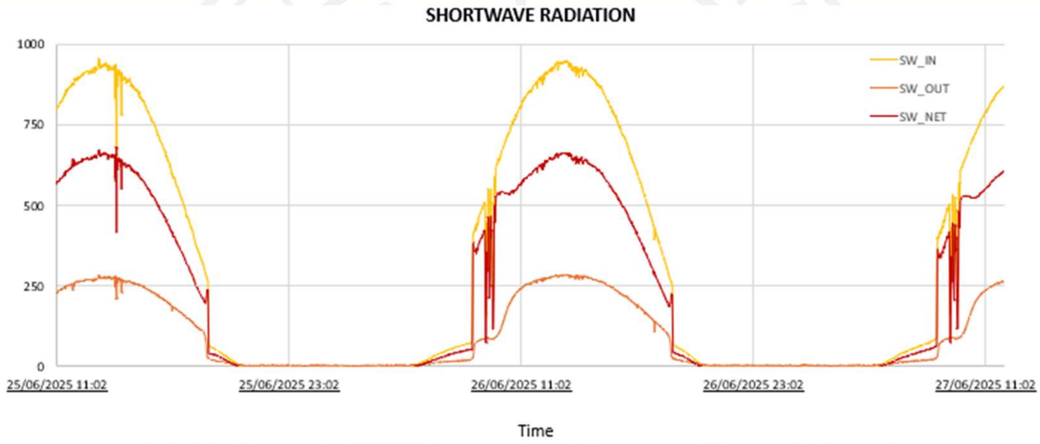

Figure 35. Shortwave radiation arriving and reflected by the pavement.

Figure 36 shows the daily trend of longwave radiation re-emitted by the pavement surface. The radiation emitted during the hottest hours of the monitored period reaches maximum values of around 78 W/m².

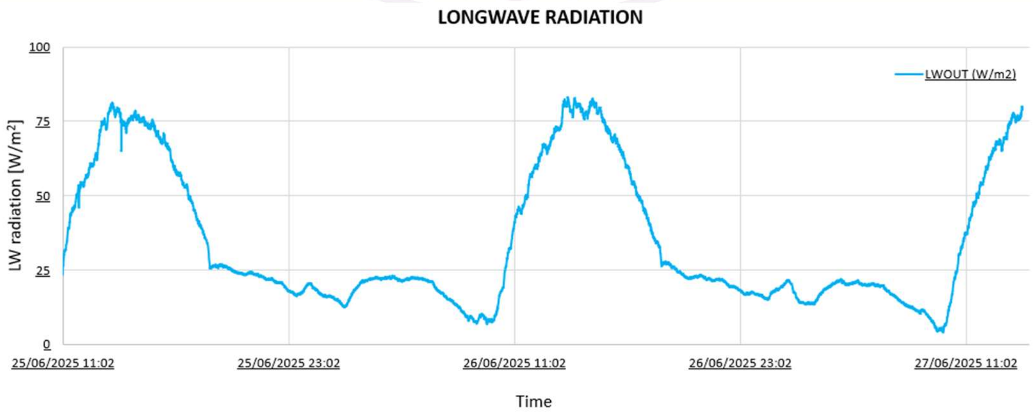

Figure 36. Longwave radiation re-emitted by the pavement.

via Duranti 93
06125 Perugia
Anna Pisello
Laura
075 585 3753
anna.pisello@unipg.it

In addition, the albedo was calculated during the central hours of the day for the monitored period, as reported in Table 17.

Table 17. Albedo

Average Albedo 25/06/2025, 12:00 – 14:00	0.29
Average Albedo 26/06/2025, 12:00 – 14:00	0.30
Average Albedo 27/06/2025, 12:00 – 14:00	0.30

The TinyTag sensors recorded surface temperature, air temperature and relative humidity, and the results are shown in Figure 37. The measured air temperature is similar to that recorded by the 4-component sensor, although slightly higher, likely due to the different positioning of the instruments: the TinyTag sensors were installed at pavement level. During the hottest central hours of the day, air temperature reached peaks of approximately 45 °C, with relative humidity between 30% and 75%. Surface temperature, on the other hand, exceeded air temperature, reaching peaks close to 55 °C during the hottest hours.

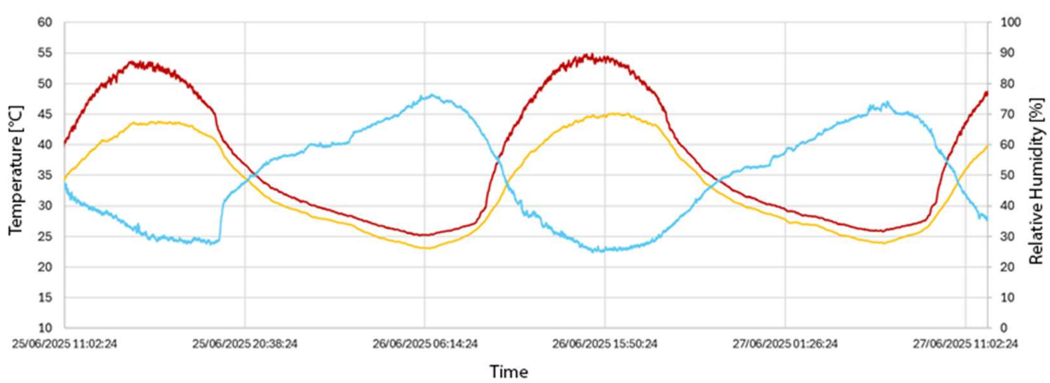

Figure 37. Data collected by the TinyTag sensors.

via Duranti 93
06125 Perugia
Anna Pisello
Laura
075 585 3753
anna.pisello@unipg.it

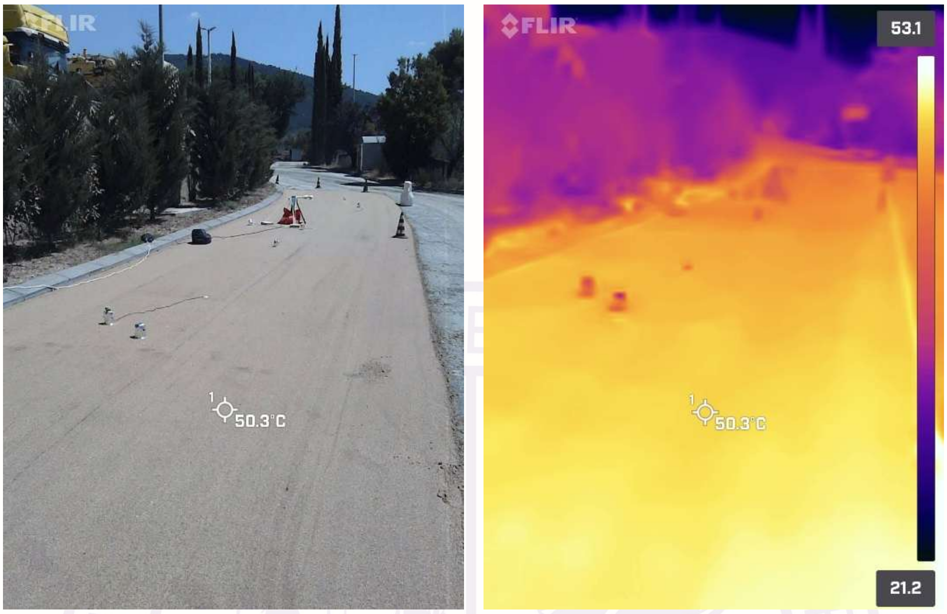

Figure 38. Test field and relative thermography.

via Duranti 93
06125 Perugia
Anna Laura Pisello
075 585 3753
anna.pisello@unipg.it

7. Conclusions

This applied research work focused on the thermo-optical analysis of four different types of high-albedo pavements with enhanced passive cooling performance, produced by POLYMERTEAM SRL, with the aim of mitigating the urban heat island effect. CIRIAF – University of Perugia was commissioned to carry out the tests necessary to characterize the supplied samples, which were produced using:

- "Bianco Ancona" aggregates + Evizero binder + 1% pigment (WHITE)
- "Bianco Ancona" aggregates + Evizero binder (NATURAL)
- "Rosso Verona" aggregates + Evizero binder (RED)
- "Bianco Ancona" aggregates + bitumen (BLACK)

In terms of combined solar reflectance and thermal emissivity, the white sample exhibits an SRI between 71 and 73, while the natural sample ranges between 57 and 60, depending on the heat transfer coefficient h_c. Both therefore comply with the requirements set by the Italian Ministerial Decree of 05/08/2024 for outdoor pavements. The red sample, starting from 30 days of ageing, also achieves an SRI between 31 and 35, thus meeting the same standard. The black sample, however, never reaches SRI values suitable for this type of application.

Consistently, the theoretical surface temperature of the black sample is always the highest, reaching up to 100 °C, while the white sample constantly shows the lowest temperatures among all samples.

In terms of thermal properties, the sample with the lowest thermal conductivity is the red one, followed by the black, natural and white samples, while the lowest thermal diffusivity is also found in the red sample. The highest volumetric heat capacity is observed in the natural sample, followed by the white one. During the ageing process, these values remain substantially stable within the experimental error range.

For use in urban pavements, materials with low thermal conductivity and diffusivity and high volumetric heat capacity tend to limit overheating of surfaces and the surrounding environment. However, other characteristics must also be considered, such as porosity, which may reduce heat capacity but promote evapotranspiration in the presence of water, also contributing to cooling. In this context, although the red

via Duranti 93
06125 Perugia
Anna Laura Pisello
075 585 3753
anna.pisello@unipg.it

sample shows the lowest conductivity and diffusivity values, the natural and white samples offer a balance between high heat capacity and light color, making them generally more suitable for areas affected by the urban heat island effect.

All intrinsic property characterization results were subsequently confirmed by thermal monitoring in a climatic chamber. During the simulation of an average summer day (climate zones B–E), the white sample remained up to 11 °C cooler than the black one, the natural sample up to 8 °C cooler, and the red sample up to 3 °C cooler. Under more extreme conditions, these differences increased: the white sample remained approximately 14 °C cooler, the natural one about 11 °C cooler, and the red one about 2 °C cooler, confirming the better thermal performance of light-colored surfaces compared to dark ones.

Finally, from the on-site environmental monitoring, the albedo of a pavement surface constructed with aggregates similar to the Bianco Ancona sample was calculated after approximately three days of monitoring. The measurements were carried out during particularly sunny and hot June 2025 days, with air temperatures reaching around 40 °C during the central hours. The pavement surface temperature reached peaks of approximately 55 °C during the hottest hours, dropping to about 25 °C during the night. From the data analysis, the albedo calculated between 12:00 and 14:00 was approximately 0.3. It should be noted that the measurements were taken less than 30 days after the pavement was laid, meaning that the surface had not yet undergone significant natural ageing. Based on the laboratory results, it is reasonable to expect an increase in optical and cooling performance over time, following prolonged exposure to atmospheric agents and the consequent natural ageing of the pavement.

via Duranti 93
06125 Perugia
Anna Laura Pisello
075 585 3753
anna.pisello@unipg.it